LANGMUIR
Cite This: Langmuir XXXX, XXX, XXX−XXX
Invited Feature Article
pubs.acs.org/Langmuir

Small Surface, Big Effects, and Big Challenges: Toward Understanding Enzymatic Activity at the Inorganic Nanoparticle−Substrate Interface

W. Russ Algar,*[,†] Tiffany Jeen,[†] Melissa Massey,[†] William J. Peveler,[†,‡] and Jérémie Asselin[†]

[†]Department of Chemistry, University of British Columbia, 2036 Main Mall, Vancouver, British Columbia V6T 1Z1, Canada
[‡]Division of Biomedical Engineering, School of Engineering, University of Glasgow, Glasgow G12 8LT, United Kingdom

Supporting Information

ABSTRACT: Enzymes are important biomarkers for molecular diagnostics and targets for the action of drugs. In turn, inorganic nanoparticles (NPs) are of interest as materials for biological assays, biosensors, cellular and in vivo imaging probes, and vectors for drug delivery and theranostics. So how does an enzyme interact with a NP, and what are the outcomes of multivalent conjugation of its substrate to a NP? This invited feature article addresses the current state of the art in answering this question. Using gold nanoparticles (Au NPs) and semiconductor quantum dots (QDs) as illustrative materials, we discuss aspects of enzyme structure−function and the properties of NP interfaces and surface chemistry that determine enzyme−NP interactions. These aspects render the substrate-on-NP configurations far more complex and heterogeneous than the conventional turnover of discrete substrate molecules in bulk solution. Special attention is also given to the limitations of a standard kinetic analysis of the enzymatic turnover of these configurations, the need for a well-defined model of turnover, and whether a "hopping" model can account for behaviors such as the apparent acceleration of enzyme activity. A detailed and predictive understanding of how enzymes turn over multivalent NP-substrate conjugates will require a convergence of many concepts and tools from biochemistry, materials, and interface science. In turn, this understanding will help to enable rational, optimized, and value-added designs of NP bioconjugates for biomedical and clinical applications.

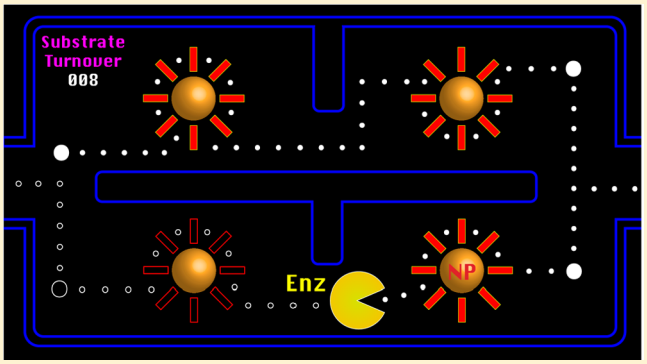

INTRODUCTION

Nanoparticles (NPs) are a diverse group of colloidal materials with dimensions between ca. 1 and 100 nm and span a wide range of properties and applications.[1] The properties of inorganic NPs are often different or enhanced versus those of the analogous bulk materials. For example, gold and other metallic NPs exhibit strong plasmonic resonances,[2] semiconductor quantum dots are brightly photoluminescent,[3] and some metal oxides and metal alloys evolve unique magnetic properties as NPs.[4] More general advantages of these materials include the combination of molecule-like diffusion with a surface area that can be functionalized, as well as large surface area-to-volume ratios. A focus of research for many inorganic NPs has been the utilization of their properties to address challenges in biology and medicine. Examples include but are not limited to cellular and tissue imaging, biosensing, drug delivery, and theranostics.[2,3,5] There is still much that needs to be learned before these ambitions can be fully realized, not the least of which is how interfacial chemistry controls the interactions between inorganic NPs and biological molecules.

Interfacial chemistry is the principal determinant of the interactions between inorganic NPs and biomolecules, and thus the optimization of surface chemistry, such as ligand and polymer coatings, has been a significant endeavor toward biomedical applications. (Here, the term *ligand* refers to a molecule that binds to the inorganic surface of a NP.) The selection of surface chemistry is not trivial as it ideally addresses several competing requirements: colloidal stability, hydrodynamic size, nonspecific interactions, and methods for bioconjugation.[6,7] Substantial effort has therefore gone into the development of coatings that tick these boxes and others depending on the details of the application. There is a sometimes-underappreciated correlation between the scope of applications for a NP material and the ease, reliability, and overall development of its surface chemistry.

A recurring theme for the surface chemistry of many NP materials is control over noncovalent interactions with biomolecules. The most common context is nonspecific adsorption or biofouling, where proteins and other biomacromolecules tend to be the chief offenders but molecules of all sizes

Received: August 10, 2018
Revised: October 4, 2018

DOI: 10.1021/acs.langmuir.8b02733
Langmuir XXXX, XXX, XXX−XXX

and types have the potential to adsorb.[8−13] The functionalization of NPs with poly(ethylene glycol) (PEG) and zwitterionic surface chemistries are common strategies for the prevention of nonspecific adsorption,[14−16] albeit that this goal is not easy to achieve. A case in point is that the protein corona that tends to form around NPs in biological fluids (e.g., blood) and in physiological environments remains a significant challenge in the translation of NPs from laboratory development to clinical application.[8,17,18] In other contexts, the goal may be an engineered interaction between a NP and a particular biomolecule of interest, for example, the cationic functionalization of a NP as a vector for gene delivery.[19,20] Whether in the context of this protein corona, engineered interactions, or adsorption in general, the noncovalent interactions of biomolecules with colloidal NPs range from low affinity, dynamic, and reversible to high affinity, static, and irreversible on the time scale of experiments, with a corresponding range of effects on biological activity and identity within a system.[8,9]

Enzymes are especially interesting from the perspective of noncovalent interactions with colloidal NPs. These catalytic proteins regulate the rates of myriad biochemical processes and are some of the most important molecular machines of life. Both the concentration and the state of an enzyme are important in determining its biological activity: the former is largely controlled via expression levels, and the latter is controlled through various mechanisms, including the proteolytic activation of proenzymes, the covalent modification of enzymes (e.g., phosphorylation), changes in the oligomerization state, and binding with small-molecule effectors and endogenous inhibitors. Enzymes are also important biomarkers for disease diagnostics (e.g., molecular assays and biosensors) and as targets for the action of drugs.[21−25] These two areas of interest are shared with NPs, so it follows that NPs are materials of interest for the detection of enzymes and their activity,[26,27] and as potential vectors for the delivery of drugs that inhibit enzymes or have their release actuated by enzymes.[28,29] Whereas the study of the adsorption of abundant serum proteins on a NP is mainly concerned with the downstream fate and function of the NP, the case of adsorption or other interactions between an enzyme and a NP necessitates concern about the fate and function of both the NP and enzyme. What are the effects of a colloidal inorganic NP and its interfacial chemistry on the activity of an enzyme? Is it possible to control and design these effects to be advantageous in applications?

Here, we review the interactions between enzymes and colloidal inorganic NPs conjugated with their substrates. That is, substrate-on-NP configurations with enzyme in bulk solution. These configurations are very useful for leveraging the favorable properties of NPs for the bioanalysis of enzymes. The converse configuration, which is enzyme-on-NP with a substrate in bulk solution, has been the topic of a greater number of fundamental studies aimed at elucidating the interactions between enzymes and NPs, including effects on catalytic activity and stability. Many of these studies have been highlighted in recent reviews.[30−32] The emphasis on how the enzyme-on-NP configuration impacts catalysis is natural given that bioprocessing and manufacturing are prospective applications of these materials.[33,34] Although studies with substrate-on-NP configurations are also numerous, most of these studies have been in the aforementioned analytical or biomedical diagnostic context: assays, sensors, and imaging probes for enzymes of biological or clinical importance. There is also interest in using NP-substrate conjugates as vectors for enzyme-mediated drug delivery. The emphasis of study has therefore been function; however, the optimization of the foregoing applications and the realization of new opportunities for substrate-on-NP configurations will require a detailed understanding of their interfacial chemistry, their interactions with enzymes, and the corresponding effects on substrate turnover.

The following sections of this article address progress and challenges toward a detailed understanding of enzymatic catalysis associated with substrate-on-NP configurations. The scope is limited to "hard" colloidal inorganic NPs, with gold nanoparticles (Au NPs) and semiconductor quantum dots (QDs) featured prominently. "Soft" organic NPs, such as those based on lipids and polymers, are also of interest for applications of substrate-on-NP configurations; however, we exclude these materials from discussion because of their markedly different chemistries and morphologies versus those of inorganic NPs. The prominence of Au NPs and QDs reflects their frequent use in fundamental studies of enzyme activity toward substrate-on-NP configurations, which follows from the reaction tracking modalities available to these materials, their well-established chemistry, and their overall breadth of prospective applications in biology and medicine. We begin by first reviewing important aspects of enzyme structure−function and important features of the colloidal inorganic NP interface. A rudimentary understanding of both NP and enzyme chemistry is assumed, and both sections are selective in their content rather than exhaustive. We then summarize methods for tracking enzyme−substrate reaction progress and address the use of the Michaelis−Menten formalism for the analysis of kinetic parameters, as well as alternative conceptual models and caveats for the interpretation of experimental data from substrate-on-NP configurations. These sections are followed by a review of the recent literature, organized by the concepts of adsorption, steric effects, interfacial environment, and the acceleration of substrate turnover. A putative hopping model of enzyme activity with NP-substrate conjugates is then critically discussed. To close, we offer a perspective on how this research will move forward and propose future opportunities for impact on applications in biology and medicine. As Figure 1 illustrates, the successful development of predictive models for the activity of enzymes toward NP-substrate conjugates will be an important advance toward these applications and a remarkable convergence of research at the intersection of biochemistry, materials science, and fundamental interface science.

■ ENZYME STRUCTURE

An enzyme potentially interacts with both components of a substrate-on-NP configuration. It is therefore useful to discuss the structural features of an enzyme that may contribute to substrate−enzyme and NP−enzyme interactions, which may occur in parallel.

The active site of an enzyme is its most famous structural feature. Introductory texts generally conceptualize the remarkably selective and efficient catalysis of enzymes through descriptions of the active site, first in terms of Fischer's "lock-and-key" model and then as the current "hand-in-glove" or induced-fit model.[35] However, the active site is not necessarily the most important structural feature of an enzyme in the context of interactions with NPs. The active site comprises a relatively small percentage of the total number of amino acid residues of an enzyme, and the number of residues that directly engage in the catalytic mechanism is typically even smaller. Serine proteases, for example, are well known for their catalytic

DOI: 10.1021/acs.langmuir.8b02733
Langmuir XXXX, XXX, XXX−XXX

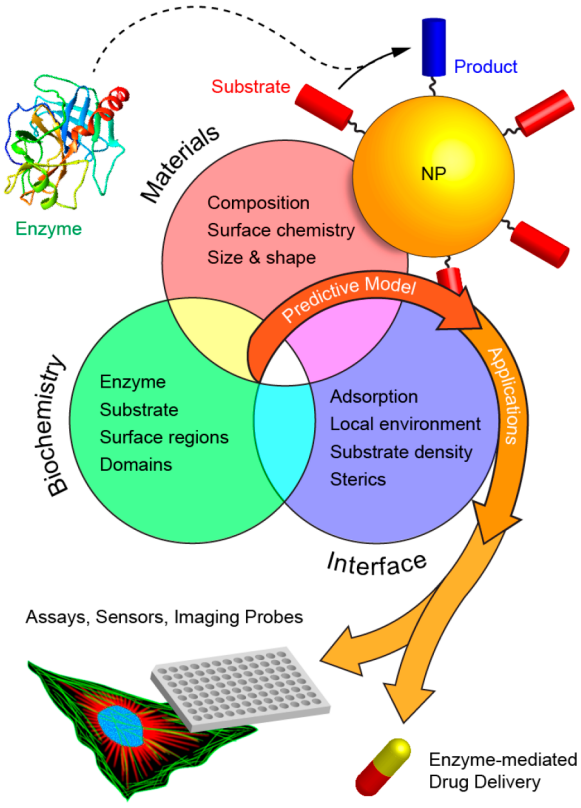

Figure 1. Graphical summary of this article. A detailed understanding of the turnover of multivalent NP-substrate conjugates by enzymes will require a convergence of biochemistry, materials, and interface science. The development of predictive models will significantly advance the applications of these conjugates, including assays, sensors, and imaging probes, as well as enzyme-mediated drug delivery.

triads of aspartate, histidine, and serine residues in the active site.[36] Chymotrypsin is a canonical example of a serine protease and has ~245 total amino acid residues, but only ~20 of these residues form the main (S1) substrate binding pocket, inclusive of the triad, and an additional 8 residues form 2 loops near the binding pocket that also play a role in determining substrate specificity.[36,37] In addition to representing a small fraction of the total amino acid residues of an enzyme, the location of the active site varies between enzymes, with some active sites at the enzyme surface and others within pockets and clefts, accessible via one or more channels of up to 2 nm or more in length.[38] Given all of the above, enzyme structure other than the active site is generally expected to predominate interactions with NPs and other interfaces. Indeed, the nonactive site structure of some enzymes evolved for the very purpose of interactions with surfaces.[39,40]

Structure away from the active site is not necessarily structure that is independent of the active site because some enzymes have allosteric sites or exosites.[41,42] Both terms refer to binding interactions at sites topologically distinct from the active site but with effects that propagate to the active site and affect the substrate turnover and specificity. These binding interactions may, for example, refer to the docking of small-molecule ligands or macromolecular ligands, dimerization of the enzyme, or association with a membrane. To illustrate structure away from the active site and highlight that enzymes have their own surface chemistry, Figure 2 shows simple ribbon and surface representations of four serine proteases: chymotrypsin, trypsin, thrombin, and plasmin. Select structural features and properties are highlighted.[37,43−50] Chymotrypsin and trypsin have orthogonal substrate specificities but have largely analogous structures except for small, but important, differences between the main binding pocket and loops.[37] Trypsin, thrombin, and plasmin share some substrate specificity in vitro but have very different structures away from the active site. For trypsin, few structural features away from its active site are noteworthy; however, thrombin has two exosites and is perhaps the best-characterized example of such an enzyme.[51,52] Plasmin has multiple kringle domains (large disulfide-stabilized multiloop structures).[44,53] The exosites of thrombin and the kringle domains of plasmin(ogen) both bind with various regulators of their activity (or activation). Given the above, it is reasonably hypothesized that the similar structures of trypsin and chymotrypsin will lead to similar interactions with NPs despite their different substrate specificities. A second hypothesis is that the distinct structural features of thrombin and plasmin will lead to quite different interactions with a NP versus trypsin, despite the ability of all three of these serine proteases to hydrolyze a common substrate by a common mechanism.

As with other proteins,[9,54] van der Waals, electrostatic, hydrogen bonding, and hydrophobic interactions, or some combination thereof, are the likely driving forces of an interaction between an enzyme and a NP. Both the surface chemistry of the NP and its size play a role, the latter determining the surface area and curvature (if the NP is approximately spherical). For a given molar concentration of NPs, more surface area offers more adsorption sites. Curvature is important because the interactions that lead to enzyme adsorption strongly depend on the distance and contact area of interaction, which must increase and decrease, respectively, as the surface of the NP falls away from a globular enzyme more quickly with a smaller diameter.[8,9,46] For an enzyme, properties such as its molecular weight, isoelectric point (pI), and solubility may be useful predictors of interactions and their magnitude but may also be oversimplifications because these properties treat the enzyme structure as homogeneous. In general, higher molecular weight correlates with more contact area for van der Waals interactions, pI indicates net charge toward electrostatic interactions, and lower solubility may portend interactions that decrease the solvated surface area of an enzyme. What is obscured by these three parameters is the potential for orientation and localization of these interactions to distinct structural features of an enzyme, for example, subunits, domains, and the aforementioned allosteric sites and exosites. As a thought experiment, imagine two enzymes with similar pI values: the first enzyme has cationic and anionic residues distributed uniformly over its surface, and the second enzyme has anionic residues uniformly distributed over its surface but has its cationic residues concentrated on only one face. The second enzyme will have much stronger electrostatic interactions with an anionic NP, which is not predicted by the similar pI values. Trypsin and thrombin are two enzymes thought to exhibit this type of difference in their interactions with anionic NPs because of the two cationic exosites of thrombin.[55] Analogously, enzymes with a scattered versus localized distribution of hydrophobic residues are anticipated to have different interactions with a NP interface.

Another aspect related to enzyme structure that warrants mentioning is steric hindrance. The context here is not the potential role of steric effects in the active site determining enzyme−substrate specificity but rather the physical size of

DOI: 10.1021/acs.langmuir.8b02733
Langmuir XXXX, XXX, XXX−XXX

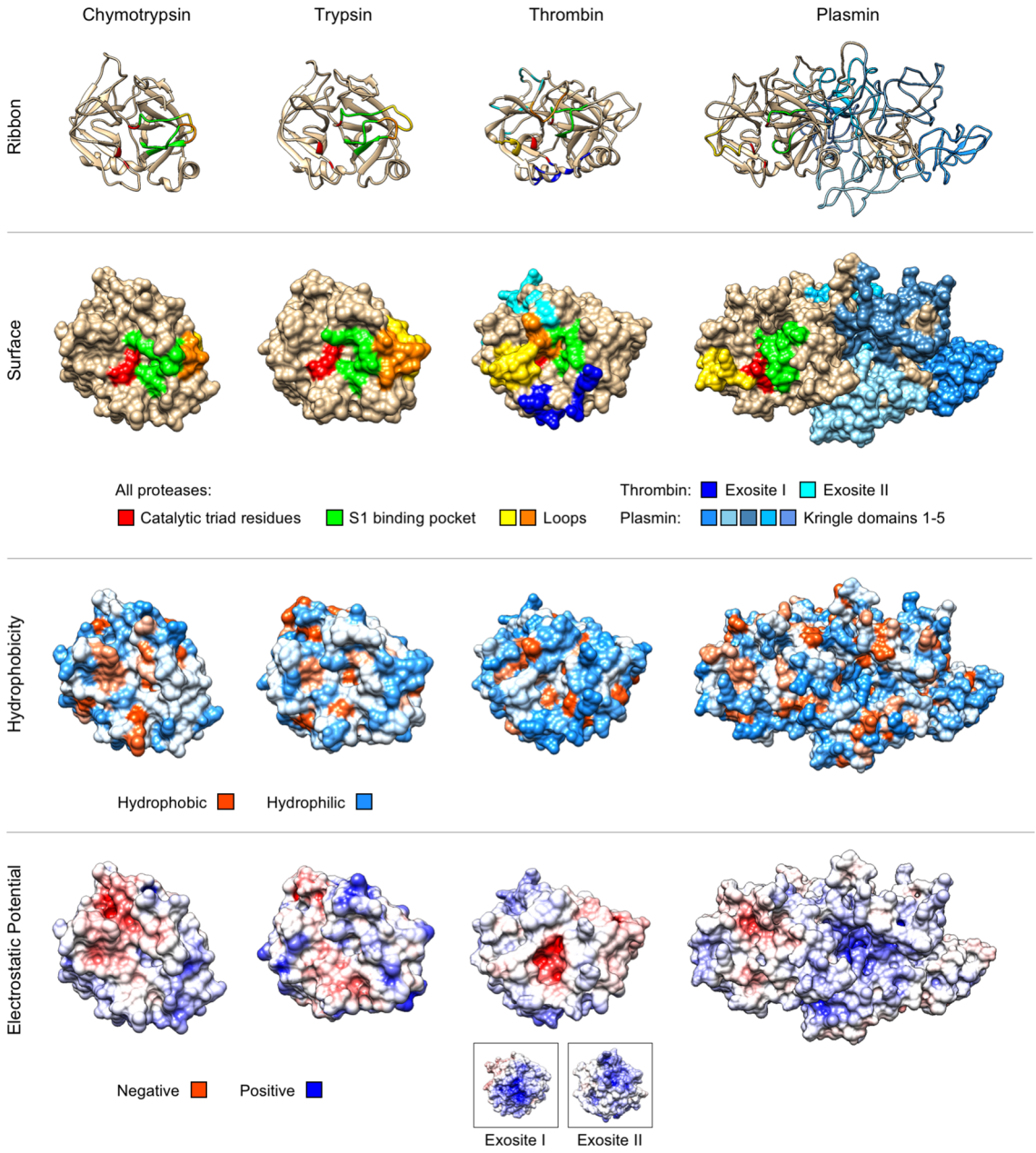

Figure 2. Ribbon and surface diagrams for the comparison of selected structural features between four members of the serine protease family: chymotrypsin, trypsin, thrombin, and plasmin. The Ser-His-Asp catalytic triads are colored red, the S1 substrate binding pockets are colored green, and select loops are colored yellow and orange. The loops for chymotrypsin and trypsin are the L1 and L2 loops, which play a role in determining substrate specificity. For thrombin, the loops are the 60-loop and the γ-loop, which contribute to substrate binding. Loop-5 is highlighted for plasmin and is most analogous to the 60-loop for thrombin. In addition, important residues for exosites I and II are highlighted in blue and cyan for thrombin, and the five kringle domains are highlighted in various shades of blue for plasmin. Surfaces that are colored according to hydrophobicity and electrostatic potential are also shown.

enzymes and NPs relative to one another and relative to the substrate. The enzymes discussed in this article range in size from 23 to 128 kDa or, if modeled as ellipsoids, have approximate dimensions of 2 nm × 2 nm × 2.5 nm up to 2.5 nm × 2.5 nm × 4 nm. The NPs are approximately spherical with diameters that range from ∼5 to ∼13 nm. It follows from these relative sizes that there is the potential for steric hindrance between the enzyme and NP that limits access to the substrate conjugated to a NP, particularly if the length of the substrate is much shorter than the radii of the NP and enzyme, or if the active site of the enzyme is located within a deep cleft.[38] Likewise, there is the potential for steric hindrance that impacts the ability of van der Waals, electrostatic, and hydrophobic interactions to occur between specific regions of an enzyme and a NP.

The takeaway message is that enzymes have size, surface chemistry, and caveats with respect to assumptions of homogeneity. Enzymes, like other proteins, also exhibit features of colloidal behavior. As discussed next, NPs are conceptually analogous in these respects. Indeed, the analogy of functionalized NPs as protein mimics has been proposed[56] because of the size and behavioral similarities.

DOI: 10.1021/acs.langmuir.8b02733
Langmuir XXXX, XXX, XXX−XXX

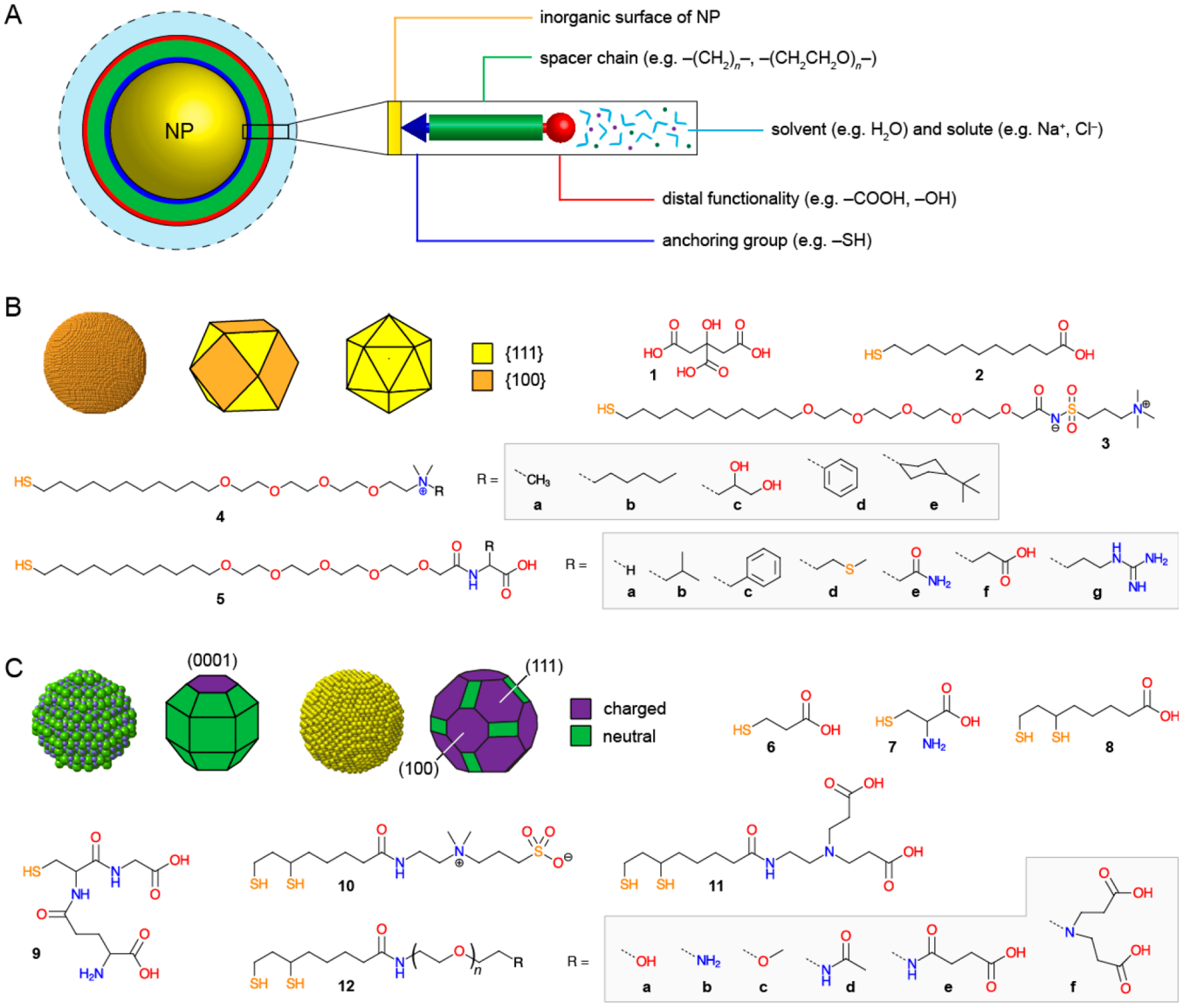

Figure 3. Aspects of the interfacial chemistry of Au NPs and QDs. (A) General structure of a ligand for functionalizing a NP and its organization at the interface of a NP. The examples of functional groups are not meant to be comprehensive in scope. (B) Cartoon of an idealized spherical 13-nm-diameter Au NP (left) and two examples of how a real crystal may be faceted (cuboctahedron, middle; icosahedron, right). Chemical structures of citrate ligand **1**, and selected examples of ligands with thiol anchors for tuning the surface chemistry, largely via the distal functionality.[62−64] (C) Cartoons of a wurtzite 3.5-nm-diameter CdSe QD (far left) and a 7-nm-diameter CdSe/ZnS (middle right), both idealized to be spherical, and two examples of how real QDs may be faceted (middle left and far right). Facets that are charged (terminated with either Cd^{2+}/Zn^{2+} or Se^{2-}/S^{2-}) or neutral (terminated with both metal and chalcogen ions) are highlighted. Chemical structures of selected examples of ligands with thiol and dithiol anchors for tuning the surface chemistry of QDs.[74−81] For **12**, the average value of n typically varies from $n = 12$ to 15. The common names of the ligands shown for both Au NPs and QDs can be found in the SI.

NANOPARTICLE INTERFACES

Colloidal Inorganic NPs. It is sometimes overlooked that the name of a NP material is, at best, a partial and ambiguous description.[57] The name defines almost nothing about the number or arrangement of atoms, whereas for a small molecule such as aspirin (acetylsalicylic acid) the name defines an exact number and arrangement of atoms of specific types. For example, the "Au NP" nomenclature indicates that gold atoms are bonded in sufficient number to form a particle with dimensions between ca. 2 and 100 nm. A variant such as "gold nanorod" indicates something about the shape. "CdSe/ZnS quantum dot" is more descriptive, indicating composition, a core/shell structure, and a size where quantum confinement effects are manifest (ca. 2−10 nm), but is nevertheless ambiguous with respect to the precise number and arrangement of atoms. Whereas a pure sample of aspirin is homogeneous, an arguably pure sample of NPs is inherently heterogeneous, starting but not ending with distributions of particle sizes and shapes (i.e., polydispersity). It is likely that the heterogeneity in size and shape propagates to heterogeneity with respect to the surface area, facets, and surface structure of each individual nanocrystal and then further propagates to the organic functionalization of each nanocrystal surface and the interface between the NP and the solvent.

Au NPs and QDs are highlighted throughout this review as two exemplars of colloidal inorganic nanocrystals and are the materials with which studies relevant to our topic have been

DOI: 10.1021/acs.langmuir.8b02733
Langmuir XXXX, XXX, XXX−XXX

most frequently undertaken. Some particular features of the structures of Au NPs and QDs are summarized in the following subsections before we return to a more general discussion of inorganic NP interfaces. Several of the features highlighted with Au NPs and QDs are also relevant to other inorganic NP materials, including but not limited to nongold metallic NPs, lanthanide-based upconversion NPs, and metal oxide and alloyed magnetic NPs. More detailed information about NP interfaces can be found in recent reviews.[7,58] Figure 3 illustrates some of the main points in the next subsections, including the general design and interfacial features of an inorganic NP functionalized with a ligand coating, cartoons of spherical Au NPs and QDs, example depictions of how real crystals may be faceted, and examples of ligand structures for tuning the surface chemistry of these two types of NPs.

Au NP Interface. Au NPs, analogous to bulk gold crystals, typically have a face-centered cubic (fcc) lattice structure.[59] Although typically approximated as spherical, crystalline Au NPs tend to be polyhedra in reality, whether Platonic, Archimedean, or Catalan.[7,60] Crystal twinning is not uncommon and leads to some of these shapes.[61] The precise shape of the NP determines the relative proportions of facets that are {111} and {100}. For example, an icosahedron has exclusively {111} facets, whereas a cuboctahedron is a mixture of eight {111} facets and six {100} facets,[7,59] albeit that surface reconstructions are expected.

Common Au NP surface chemistries include citrate ligands, polymers, and discrete thiol(ate) ligands.[6] Citrate can be convenient to retain from synthesis but is often a poor or mediocre ligand in many applications because of its weak binding and tenuous electrostatic colloidal stabilization of the Au NP. Thiol(ate) ligands with distal hydrophilic groups tend to be the most common and effective strategy in applications that require control of surface chemistry. These ligands include both small molecules and biomacromolecules such as oligonucleotides terminated with a thiol linker. As an example of the former, the Rotello group has developed an impressive library of small-molecule ligands for Au NPs with tunable distal functionality that has been shown to modulate protein−NP interactions.[62−64] Pioneered by the Mirkin group, the multivalent functionalization of citrate-stabilized Au NPs with oligonucleotides has been the foundation of several bionanotechnological advances and the foundation of a proposed class of materials called spherical nucleic acids.[65]

Thiols are well known for their strong binding to metallic gold; however, the precise modes of binding remain under scrutiny.[66−69] The putative binding modes between thiol ligands and Au NPs are inferred from studies on bulk planar gold interfaces and with atomically precise gold nanoclusters. The original model of thiols binding at 3-fold hollow sites on an unreconstructed planar gold {111} surface to form $\sqrt{3} \times \sqrt{3}$R 30° lattices and $c(4 \times 2)$ superlattices has been challenged by the observation of monomeric RS−Au_{ad}−SR and dimeric RS−$(Au_{ad}-SR)_2$ "staple" binding motifs and Au−SR−Au bridge-site binding motifs, largely but not exclusively with nanoclusters.[66,67,69,70] Experiments suggest that staples are associated with adatoms and are preferred on {111} facets, whereas bridge binding may be preferred on {100} facets.[68,71,72] The process of adsorption of thiol ligands on gold surfaces can also induce surface reconstructions[66,70] such that the inorganic component of the interface is not necessarily static. The complete implications for Au NPs remain to be determined, but it is reasonably anticipated that there will be a size- and facet-dependent distribution of thiol−gold binding motifs.

QD Interface. Like Au NPs, QDs are typically approximated as spherical but are also polyhedra, with the numbers and types of facets determined during nanocrystal synthesis.[7,58] CdSe is the prototypical QD material and can adopt both zinc blende and wurtzite crystal structures. Zinc blende QDs tend to be tetrahedral or faceted in a way that approximates a sphere, with the possibility of being isotropic and displaying only one type of facet, whereas wurtzite QDs tend to be slightly elongated along their *c* axis and are multifaceted.[58] Ultimately, the shape of the QD nanocrystal determines the facets displayed, where these facets can be cationic and terminated with Cd^{2+} ions with coordination number 2 or 3, anionic and terminated with Se^{2-} ions, or neutral and terminated with both Cd^{2+} and Se^{2-} ions, albeit that surface reconstructions are expected. Although the foregoing is written in the context of CdSe QDs, the general concepts extend to many common core QD materials, including other II−VI semiconductors such as CdS and ZnS, III−V semiconductors such as InP, IV−VI semiconductors such as PbS, and epitaxial core/shell QD structures such as CdSe/ZnS.

Hydrophilic QDs are typically functionalized with one of three general chemistries: discrete ligands that bind to the inorganic nanocrystal, polymers with pendant groups that bind to the inorganic nanocrystal, and amphiphilic polymers that wrap around the nanocrystals and retain hydrophobic ligands from synthesis.[6,73] For studies of enzyme activity toward QD-substrate conjugates, discrete ligands based on anchoring thiol(ate) groups and distal hydrophilic groups have been the most common type of surface functionalization. Figure 3 shows several examples of thiol ligands, including a family of ligands based on dihydrolipoic acid (DHLA) and a subset of DHLA-PEG ligands with various distal functional groups.[74−81] Many of these ligands are from or are inspired by the Medintz and Mattoussi groups.[74−79]

The thiol(ate) groups of ligands preferentially bind to cationic sites on the nanocrystal surface,[7,58] and therefore different densities and displays of ligands are anticipated between facets. In principle, the same ligands can be used to functionalize Au NPs and QDs; however, the coordinate bonding interactions between thiol(ate) ligands and cationic sites on the QD surface are weaker than the corresponding bonding interactions with Au NPs. This fact accounts, in part, for the predominance of monothiol ligands with Au NPs and dithiol ligands based on DHLA with QDs.

Interfacial Heterogeneity. It emerges from the previous subsections that nanocrystals are not only heterogeneous in size and shape but also potentially heterogeneous as individual particles because of their different facets. Differences in inorganic structure between facets are anticipated to propagate to differences in organic ligand displays between facets, with the ligand numbers and densities being two such examples. These differences may have downstream effects as, for example, density contributes to the frequency of gauche defects, as does the radius of curvature of a NP.[7,82,83] Ligands fan out as the radius of curvature decreases and thus more space is available to accommodate gauche defects. With the idea that facets are locally flat faces of a nanocrystal, the concept of the radius of curvature translates into the total numbers and size of each facet and breaks in ligand coverage at edges and vertices between facets, which accommodate a large amount of structural disorder. The structural disorder is generally expected to decrease as the facets grow larger and with features of a ligand that promote better packing (e.g., longer alkyl chain lengths). Surface reconstructions induced by ligand adsorption are

DOI: 10.1021/acs.langmuir.8b02733
Langmuir XXXX, XXX, XXX−XXX

anticipated to add to the differences between facets, perhaps to the point that no two facets in an ensemble of NPs are truly equivalent.

Even more heterogeneity may be encountered in the special case of core/shell NPs because the epitaxial growth of a uniform shell is not trivial. The possibility of uneven or incomplete coverage with shell material, which has been observed with core/shell QDs,[84] brings with it the possibility that different facets have different chemical compositions. Likewise, if ligand exchange is used to apply the final organic coating to a NP, then this process is not necessarily 100% efficient or uniform between different facets[85,86] and is another potential source of heterogeneity in chemical composition between facets.

Yet another source of interfacial heterogeneity is bioconjugation, which, for example, is required to attach an enzyme substrate to a NP. The concepts and challenges of NP bioconjugation have been reviewed in detail elsewhere.[1] For many chemistries, both the NP and the biomolecule of interest have multiple potential points of attachment, which generally results in a population of NP-bioconjugates with broad distributions in the number of biomolecules per NP and the orientations of those biomolecules. The tendency of hydrolysis to compete with many popular bioconjugation reactions exacerbates the challenge and adds potentially significant batch-to-batch variation. Although some chemistries provide much better control and reproducibility than others (e.g., the self-assembly of polyhistidine-tagged and thiol-terminated biomolecules to QDs and Au NPs, respectively), there are few, if any, chemistries that enable the conjugation of biomolecules to QDs and Au NPs in a manner that is homogeneous in number and attachment point per NP.

There is no all-in-one characterization method for the NP interface. Instead, an array of methods must be utilized and cross-referenced, often with great attention to detail to correctly identify and interpret features in the data.[7,87,88] Consequently, many of the above concepts are not yet directly characterized or fully understood but rather are inferred from an accumulation of experiments and observations, or extrapolated from cluster molecules or related bulk materials.

Sources of Interfacial Variability. To this point, fundamental materials chemistry has been discussed as a root cause of heterogeneity. A related challenge is the variability between preparations of NPs. Although batch-to-batch variation is also rooted in chemistry, it is not just an outcome of the nominal identity of the NP material but also an outcome of the detailed route by which the NP material was attained. Synthesis factors that are expected to affect the details of a final inorganic NP include the selection of precursors, solvents, and ligands; impurities; reagent stoichiometry; mixing/stirring efficiency; and temperature, pressure, and pH, among other conditions.[89−94] For example, the practical challenge of precisely regulating high temperatures and reagent impurities in the early solvothermal synthesis of QDs was (and remains) a considerable source of variability, as are the conditions of shell growth. In addition, aqueous and solvothermal methods of synthesis for compositionally identical QD materials (e.g., CdTe, CdS) do not tend to yield functionally equivalent materials.

The above arguments regarding reactants and reaction conditions also extend to surface functionalization methods such as ligand exchange. Given that ligand adsorption may induce surface reconstruction, it is not necessarily the case that the initial inorganic surface is immutable during ligand exchange. It is thus possible that the *combination* of methods for NP synthesis and ligand exchange determines the density, orientation, and other details of the final ligand-functionalized NP interface.

In addition to all of the above, the aging of inorganic NP materials is another potential source of heterogeneity. For example, some NP materials, including QDs, are susceptible to oxidation and the formation of an oxide layer at their interface.[95] Corrosion, etching, and leaching are general degradation pathways for most metal-based NPs, with the rates of degradation being dependent on the materials and their passivation and conditions such as temperature and pH. As an example, silver NPs are notorious for their poor chemical stability, which stands in contrast to the comparatively good stability of Au NPs.[96] Ligands are also a potential source of aging because noncovalent binding makes their off-rate and desorption equilibrium important once a functionalized NP is purified of excess ligand. The off-rate and position of a new equilibrium between free and bound ligand will depend upon the dilution, the strength of the ligand−NP binding interaction, and the pH or other conditions that affect that interaction.[97,98] The foregoing discussion also extends to conjugated biomolecules, which may desorb if bound noncovalently (including covalent bonding to noncovalently bound NP ligands) and denature or otherwise degrade over time. Irrespective of material and mechanism, the rapid, severe degradation of a NP material is perhaps a minimal source of variability because it is readily detected. It is slower degradation over days, weeks, or months with minimal outward symptoms that may be more problematic over a series of experiments.

Overall, the variability between the final NP materials produced by different methods and between batches produced by the same nominal method is an obstacle to a more detailed understanding of how NP surface chemistry affects downstream applications. Thorough, detailed reporting of methods is essential for published reports, and guidelines for the detailed characterization of NPs have been proposed to help compare and reconcile observations between different studies and batches of materials; however, the undertaking is nontrivial, and most studies tick only some of the boxes.[87,99−101]

Interfacial Environment. The full interfacial environment of a NP comprises not only the inorganic nanocrystal surface and its organic ligands but also conjugated biomolecules (e.g., peptides and other enzyme substrates) and local solvent and solute molecules.

The local volume of solvent generally differs from that of bulk solution (i.e., far from the NP) as there is a reorganization of solvent within ∼2 nm of a NP interface.[102] This reorganization varies between anionic and cationic, zwitterionic, and hydrophilic neutral coatings (e.g., PEG) on a NP, and indeed, the details of hydration and hydrogen bonding are principal factors in the nonfouling character of PEG and zwitterionic coatings.[103,104] Charge at the NP interface also brings about the well-known electrical double layer, resulting in a different local ionic strength at the NP interface. The Debye length ranges from less than 1 nm to several nanometers depending on the bulk ionic strength.[105]

Other important considerations at the NP interface arise from multivalency, which refers to the numbers of ligands and conjugated biomacromolecules per NP. Nearest-neighbor interactions occur with some similarity to bulk interfaces but also with potential differences from the radius of curvature or faceting of a NP. As an example of interactions between ligands, the carboxyl group pK_a of monothioalkyl acid ligands is elevated

DOI: 10.1021/acs.langmuir.8b02733
Langmuir XXXX, XXX, XXX−XXX

on Au NPs and QDs because of hydrogen bonding between adjacent ligand molecules, mediated in part by the radius of curvature of the NP.[106,107] The same effect does not appear to be observed with dihydrolipoic acid ligands, presumably because of different organization and density imposed by their dithiol anchoring group. A high local concentration of conjugated biomolecules can also induce concentration-dependent processes to occur efficiently at the interface of a NP even when inefficient in bulk solution. To illustrate, imagine a NP of diameter d, conjugated with an average of N peptides per NP, where a distance of 10 nm from the NP surface is (arbitrarily) defined as the local environment. Figure 4 plots the

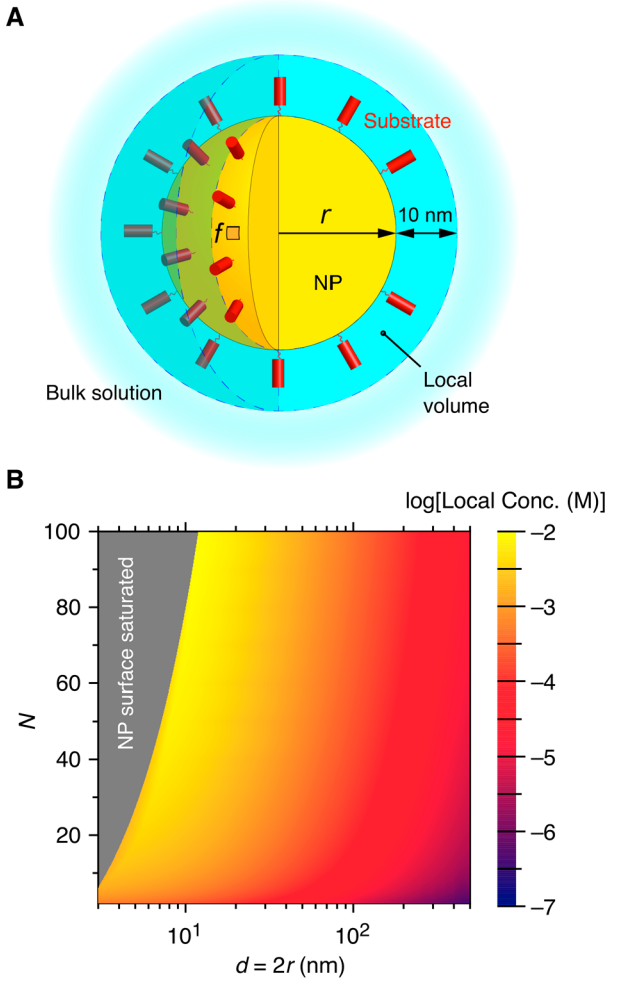

Figure 4. High local concentration of a substrate around a NP. (A) Simple model of a NP-$[\text{substrate}]_N$ conjugate: the NP has a radius r, and there are N substrates per NP that occupy a local volume that extends radially 10 nm from the NP surface. The saturation of the NP surface is based on a footprint of $f \approx 4$ nm^2 for each substrate. (B) Plot of the local concentration as a function of NP diameter and the value of N. Details of the calculation can be found in the SI.

concentration of peptide within this volume depending on the value of N and the diameter of the NP. The local concentration varies by 3 orders of magnitude from ~10 μM to ~10 mM. One example of a demonstration of this effect is the self-quenching of fluorescence from QD-conjugated, dye-labeled peptides because of dimerization of the dyes between neighboring peptides.[108] No such behavior was observed without the localization of multiple copies of the peptide to a QD. This result also suggests the potential for dimerization or other density-induced interactions between conjugated biomolecules themselves.

Note that there is a distinction between the concepts of a high local concentration and high avidity for a NP.[54,109] In our context, effects from a high local concentration are associated with an increased probability of productive encounters between an enzyme and substrate at a NP interface, whereas effects from avidity are associated with multiple, concurrent binding interactions (e.g., multiple biomolecules conjugated to the same NP are bound to multiple receptors on a cell membrane). A single enzyme with a single binding site does not experience avidity with respect to the NP because it can bind only to a single substrate molecule at any given time.

Another effect from the multivalent conjugation of biomacromolecules to a NP is a reduction in their degrees of freedom versus the bulk solution because of their anchoring and interactions (e.g., steric, electrostatic) with the surface of the NP and between one another, which impacts the range and dynamics of conformations adopted. For example, oligonucleotides and peptides adopt an average conformation that is more upright as their number per NP increases.[110,111] Moreover, the radius of curvature of a NP affects the maximum densities of conjugated biomacromolecules that can be achieved, with smaller-diameter NPs supporting a smaller number but higher density because of the greater deflection angle between nearest neighbors.[112] The density of biomacromolecules on a NP can therefore be greater than on a bulk interface.

The next section will review how measurements of the enzymatic turnover of NP-substrate conjugates are made, and, in part, will highlight how conventional analyses overlook or homogenize much of the detail and heterogeneity discussed in this section.

METHODS AND MODELS

Assay Methods. The most common methods for tracking enzyme activity toward NP-substrate conjugates are based on fluorescence. These methods capitalize on the inherent photoluminescence (PL) properties of QDs and the fluorescence quenching abilities of Au NPs.[113] Fluorescence methods are very useful for tracking enzyme activity because they are sensitive, multicolor, and, in the cases of Förster resonance energy transfer (FRET) and electron transfer quenching, enable real-time tracking without washing or developing steps. Real-time tracking is also advantageous because it allows the enzyme−substrate reaction to be followed with high temporal resolution. Suitable calibration also enables quantitative measurements. These methods are robust but nevertheless work best when care is taken to minimize artifacts from strong light scattering, inner filter effects, and trivial radiative energy transfer. The desired data from tracking is a measure of the substrate or product as a function of time—a partial or full reaction progress curve.

The substrate selected for an assay must concurrently satisfy the criteria mandated by the specificity of the enzyme and support a mechanism of signaling upon its turnover to product. (See the SI for more discussion.) Dye-labeled substrates are a common strategy for tracking hydrolase activity with Au NPs and QDs. For example, dye-labeled peptides are useful for tracking protease activity.[114,115] The dye initially quenches the QD PL emission intensity via FRET, and peptide hydrolysis is tracked through the recovery of QD PL as the dye diffuses beyond the range of energy transfer. If this dye is fluorescent, then the ratio of dye and QD PL emission intensities is another

DOI: 10.1021/acs.langmuir.8b02733
Langmuir XXXX, XXX, XXX−XXX

useful metric for tracking. An analogous format substitutes an Au NP for the QD, where the fluorescent dye label on a conjugated peptide is quenched via energy transfer to the Au NP and the recovery of dye fluorescence emission intensity tracks with the hydrolysis of the peptide.[116] These two formats are equally applicable to nucleases with the substitution of an oligonucleotide for the peptide[117−122] and, in principle, to all types of hydrolases and their macromolecular substrates. Tracking of transferase activity is also possible using a similar assay format. The distinction for transferases is that the enzyme does not cleave the fluorescent dye from the NP-peptide substrate conjugate but rather modifies a specific peptide residue with the dye, either directly or indirectly.[123−125] Direct modification is usually preferable for real-time kinetic measurements. Figure 5 summarizes the foregoing energy-transfer-based assay formats, which may also prove useful for tracking ligase and lyase activity.

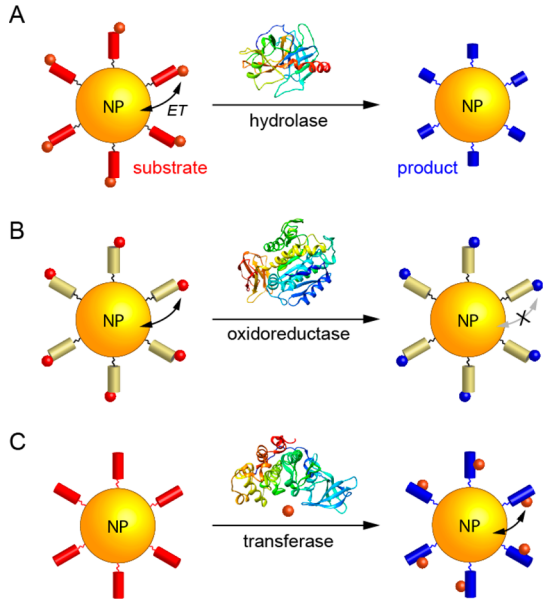

Figure 5. Examples of energy transfer (ET)-based (e.g., FRET, electron transfer) assay formats for tracking enzymatic activity toward NP-substrate conjugates. (A) Release of an energy transfer partner from a NP through cleavage of a labeled substrate by a hydrolase. (B) Conversion of a label from an energy transfer-active form to an inactive form (or vice versa, not shown) by an oxidoreductase. (C) Labeling of a substrate with an energy transfer partner by a transferase. In principle, assay formats similar to those in panels A and C can be used for tracking lyase and ligase activity.

Analogous in concept to the above, there are some cases where the product itself quenches the QD PL emission via FRET or electron transfer but the substrate does not (or vice versa). This format requires that the substrate changes color upon conversion to product in order to modify the spectral overlap parameter required for FRET or that it changes its redox properties in order to modulate quenching by electron transfer.[123,126] These configurations tend to be most useful with oxidoreductases.

If FRET and electron-transfer quenching are not practical, then the tracking of enzymatic activity may, in principle, be achieved through chromogenic and fluorogenic small molecules[127,128] conjugated to NPs as substrates for an enzyme of interest. Here, the signal for tracking enzyme activity is independent of the Au NP or QD. These substrates are widely utilized for general assays of enzyme activity and have frequently proven useful with enzyme-on-NP configurations (for example, refs 129−131) but have not been common with substrate-on-NP configurations. There is no fundamental limitation for the latter as resolving changes in color or fluorescence intensity versus a background of Au NPs or QDs has been feasible with enzyme-on-NP configurations. It is simply that there is little precedent for this assay format because the use of a chromogen or fluorogen in parallel with a Au NP or QD is redundant from the standpoint of detection. Nevertheless, the format may prove useful as the scope of fundamental studies on substrate-on-NP configurations expands to more enzymes with nonmacromolecular substrates.

Returning to FRET assay formats, a potential challenge in assaying hydrolase activity toward substrate-on-NP configurations is the nonspecific adsorption of product on the NP,[55,115] typically driven by electrostatic or hydrophobic interactions. The culprit may be the substrate itself or the dye label that engages in energy transfer. The result is that the signal for tracking substrate never goes to zero energy transfer efficiency, which is otherwise expected for complete conversion to product. Calibration methods to help account for adsorption have been proposed and are discussed in the next subsection,[115,132] but nonspecifically adsorbed product fragments remain difficult to distinguish from a subpopulation of putative substrates that are inactive or inaccessible.

Another challenge in assays is drift, which may take the form of drift in instrument response, drift in the chemistry of the NP-substrate system (e.g., photobleaching or other nonenzymatic degradation causing a slow change in the measured observable), and drift in the activity of the enzyme (e.g., denaturation or other degradation over time). It is important that each of these forms of drift is evaluated and addressed through control experiments.

A third and occasional challenge in assays is the measurement of a NP-free, substrate-only control experiment. Either an altogether different method must be used (e.g., a separation method)[55,115,133] or a fluorescent dye or molecular quencher is introduced to replace the QD or Au NP.[121,122] Although there are good examples of both approaches, neither is trivial. For example, in our hands, the former approach has been laborious and required a honed technique to avoid poor precision, and the latter strategy has been less reliable with peptide substrates than with oligonucleotide substrates because of a greater propensity for dye−dye interactions with the dual labeling of a peptide. One must also consider the possibility that interchanging between NP and dye alters a property of the substrate (e.g., average conformation) that convolves with the desired loss of effects from the NP to alter the apparent enzymatic activity. The hypothetical use of small-molecule chromogenic or fluorogenic substrates avoids these potential challenges.

Progress Curves and Michaelis−Menten Analysis. The data obtained from assays are full or partial reaction progress curves that represent the rate of conversion of substrate to product. The raw data is typically in the form of fluorescence intensity versus time. Obtaining a turnover rate in standard units ($M\ s^{-1}$) requires a calibration to convert the progress curves to a molar quantity versus time, as detailed in the next subsection. The reflexive kinetic analysis tends to be the Michaelis−Menten (MM) model for extracting the parameters K_M and k_{cat}, the Michaelis constant and turnover number, respectively, and their ratio, k_{cat}/K_M, which is the specificity constant. The appeal is that the MM parameters are the familiar and basic quantitative language of enzymology; however, as elaborated on below, the

DOI: 10.1021/acs.langmuir.8b02733
Langmuir XXXX, XXX, XXX−XXX

model tries to standardize the results from configurations that are nonstandard and assumes homogeneity. The formalism thus has deficiencies for NP-substrate conjugates.

Two methods are principally used to arrive at values for the MM parameters from progress curves: calculation from initial rates, per eq 1, or the fitting of full progress curves with the integrated MM equation, per eq 2. The terms in these equations are the reaction velocity, v, and the concentrations of substrate and product, [S] and [P], as a function of time, t, where the naught subscript denotes an initial value and the t subscript denotes a value at an arbitrary time point. Equation 3 is the closed-form solution of eq 2, where W is the Lambert function.[134−137]

$$-\frac{\mathrm{d[S]}}{\mathrm{d}t} = \frac{\mathrm{d[P]}}{\mathrm{d}t} = v = \frac{k_{\mathrm{cat}}[\mathrm{E}]_0[\mathrm{S}]}{K_{\mathrm{m}} + [\mathrm{S}]} \tag{1}$$

$$K_{\mathrm{m}} \ln\left(\frac{[\mathrm{S}]_0}{[\mathrm{S}]_t}\right) + [\mathrm{S}]_0 - [\mathrm{S}]_t = k_{\mathrm{cat}}[\mathrm{E}]_0 t \tag{2}$$

$$[\mathrm{S}]_t = K_{\mathrm{m}} W\left\{\frac{[\mathrm{S}]_0}{K_{\mathrm{m}}} \exp\left(\frac{[\mathrm{S}]_0 - k_{\mathrm{cat}}[\mathrm{E}]_0 t}{K_{\mathrm{m}}}\right)\right\} \tag{3}$$

The MM model in eqs 1−3 has several implicit assumptions and guidelines: a large excess of substrate in order to achieve the Briggs−Haldane or steady-state approximation of $\mathrm{d[ES]}/\mathrm{d}t = 0$,[138] where ES is the enzyme−substrate complex; the free ligand condition of $[\mathrm{E}]_0 \ll K_{\mathrm{m}}$; and $[\mathrm{S}]_0 \gg 3K_{\mathrm{m}}$ to determine K_{m} and k_{cat} separately rather than as only the specificity constant.[136,137] Moreover, the enzyme must be stable over the period of measurement, the reaction must be irreversible and without product inhibition, and progress curves for a series of enzyme concentrations should pass Selwyn's test and follow a single trajectory when plotted in enzyme time.[139]

For eq 1, initial rates can be obtained from tracking over a time window that corresponds to the initial turnover of substrate (typically a few percent consumption or less) or from the mathematical fitting of full progress curves. In the latter case, the equation for fitting can be empirical and need not be the integrated MM equation, but eq 1 and eqs 2 and 3 should ultimately yield the same values for K_{m} and k_{cat} in the absence of deviations from MM behavior.

Even if the initial rates will be the basis of quantitative analysis, we recommend the measurement of full progress curves. Almost every reaction progress curve looks the same in its initial stages: approximate linearity at short times and negligible substrate consumption followed by the introduction of modest curvature at somewhat longer times as the substrate begins to be depleted. Substantial consumption of substrate is needed to test the validity of a kinetic model and resolve mechanism differences. Figure 6A shows an example of how the measurement of only the initial portion of the progress curves would completely obscure two different kinetic profiles. This mock data is inspired by a real example (vide infra) where the differences between the initial and full progress curves revealed key differences in the models of substrate turnover with a NP.[133] Of course, it is obvious in this example that a naïve assumption of the MM model is inappropriate and that a full progress curve is useful. There are also more subtle examples, including our finding that the turnover of multivalent QD-peptide substrate conjugates by a protease did not strictly follow the MM model.[115] Figure 6B shows some of this data, where the deviations are the poor fit of

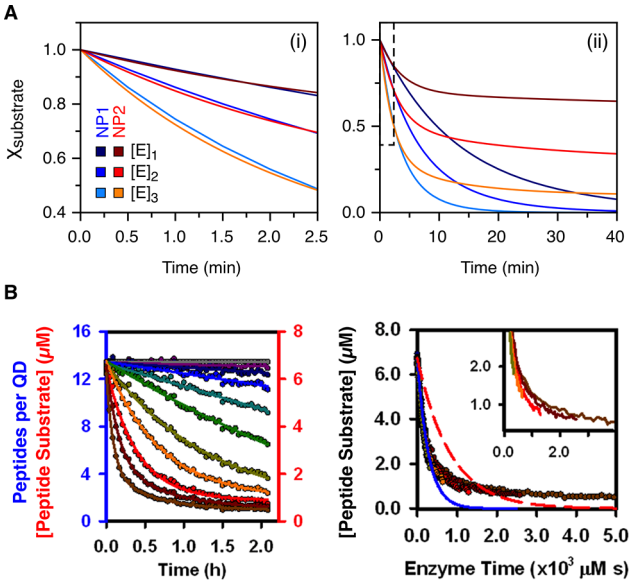

Figure 6. (A) Hypothetical progress curves for the enzymatic turnover of NP-$[\mathrm{substrate}]_N$ conjugates with two different NP materials and three enzyme concentrations. Measurement of only (i) the initial rates does not reveal significant differences between the two NP materials, whereas the measurement of (ii) full progress curves clearly reveals differences. The dashed box in panel ii indicates the region in panel i. (B) Kinetic data for the turnover of QD-$[\mathrm{peptide\ substrate}]_{13}$ conjugates by trypsin: (left) standard progress curves for different concentrations of trypsin (0, 1.3−687 nM, scaling by a factor of 2 from purple to red) and (right) progress curves plotted in enzyme time. The blue line is the best fit to the MM model. The red line is the MM prediction from assays of substrate only. The inset shows a close-up of data early in the progress curves. Reproduced from ref 115. Copyright 2012 American Chemical Society.

the modeled MM progress curve and the lack of a single trajectory when the experimental progress curves are plotted in enzyme time.

In addition to the fit of the data, it is also important to consider the congruity between the assumptions of the MM model and the conditions of the experiment. The MM formalism sometimes presents challenges for substrate-on-NP configurations because NPs are typically used at submicromolar concentrations and thus a large excess of substrate over enzyme may be impractical to achieve. Although there is a reformulation of the MM formalism for excess enzyme,[140,141] the situation is complicated by the potential for concurrent turnover of multiple substrates on a NP by multiple enzymes. An alternative approach that has been adopted with a small excess of substrate is the determination of the specificity constant, $k_{\mathrm{cat}}/K_{\mathrm{m}}$, as a single value with the subsequent estimate of K_{m} via the assumption that k_{cat} is unchanged from assays with substrates but not with NPs.[115,126]

Beyond technical challenges, there is a more fundamental question to answer with respect to the applicability of the MM model: what does [S] represent for a substrate-on-NP configuration?

The number of diffusing entities in an x M solution of NP-$[\mathrm{substrate}]_N$ conjugates (i.e., N substrates conjugated per NP) is less than in an equal volume of Nx M solution of substrate alone, but the number of substrates that can be converted to product is greater for x M NP-$[\mathrm{substrate}]_N$ conjugates than for x M substrate alone (notwithstanding the frequent challenge of measuring x accurately for samples of NPs). The choice of [S] =

DOI: 10.1021/acs.langmuir.8b02733
Langmuir XXXX, XXX, XXX−XXX

x M or [S] = Nx M becomes important for quantitative comparisons of K_m and k_{cat} between different studies and for comparisons between assays with NP-[substrate]$_N$ and substrate only, where the potential factor of N difference in these parameters needs to be explicit lest it affect the conclusions drawn. As will be detailed in the next section, the proposed model of turnover for NP-[substrate]$_N$ conjugates may also influence the choice of [S] = x M or [S] = Nx M. There is a proposed hopping model where the conjugate undergoes single-step conversion from NP-[substrate]$_N$ to NP-[product]$_N$ in an encounter with enzyme. If this model is accepted, then the logical interpretation is that [S] = x M and each value of N for the conjugate represents a unique substrate that, in principle, has its own values for K_m and k_{cat}. In any case, derived values for K_m and k_{cat} are best labeled as "apparent" but have utility for comparison between different multivalent NP-substrate conjugates.

Given the above, an MM analysis should not be automatic. Its use should be accompanied by clear statements of assumptions and an evaluation of how a change in assumptions would (if at all) impact the conclusions drawn.

A more general approach to kinetic analysis is stepping back to collision theory. There are interpretations of enhancements of enzyme activity associated with NP-substrate conjugates that point to parameters such as the collision cross-section and steric factor,[31] and these parameters may be sufficient if single-step conversion of NP-[substrate]$_N$ to NP-[product]$_N$ is accepted. If not accepted, modifications to collision theory should take into account that multiple productive collisions are needed to convert all N substrates per NP into product. More detailed models may also seek to tease apart potential enzyme–substrate and enzyme–NP interactions and allow for distributions of values for model parameters that arise from nontrivial polydispersity or other heterogeneity of a NP sample. A more detailed look at the mathematics for models based on collision theory can be found elsewhere,[31] and we will later address conceptual factors for these models in the context of the capacity for NP-substrate conjugates to accelerate enzymatic activity.

Model Matters. With the questionable applicability of a simple MM model, other models are needed for the interpretation of progress curve data. As noted earlier, a hopping model has been proposed for the enzymatic turnover of NP-substrate conjugates.[55,115,133] In this model, all of the substrate conjugated to an individual NP is hydrolyzed in a single encounter with a single enzyme. The putative rate-limiting step is the diffusion of the enzyme between NPs. The opposite extreme is a model where only one of the conjugated substrates is hydrolyzed per encounter between an enzyme and the NP, which we call the "colliding" model.[115] For this model, the putative rate-limiting step is enzyme–substrate binding. Figure 7 illustrates the difference between these two models in terms of the time-dependent distribution of the number of substrates per QD, assuming simple Poisson statistics.[142] The colliding model, which invokes a series of discrete enzyme–substrate interactions, is conceptually most similar to the conventional MM model, but the hopping model is the most congruent mathematically. The following paragraphs will illustrate how the results of a quantitative analysis of experimental data can depend on the model with which the data is interpreted.

As a thought experiment, consider an assay for protease activity with QD-[substrate–dye]$_N$ conjugates and the use of FRET for tracking substrate hydrolysis. Figure 8A shows hypothetical progress curves for this experiment, which are

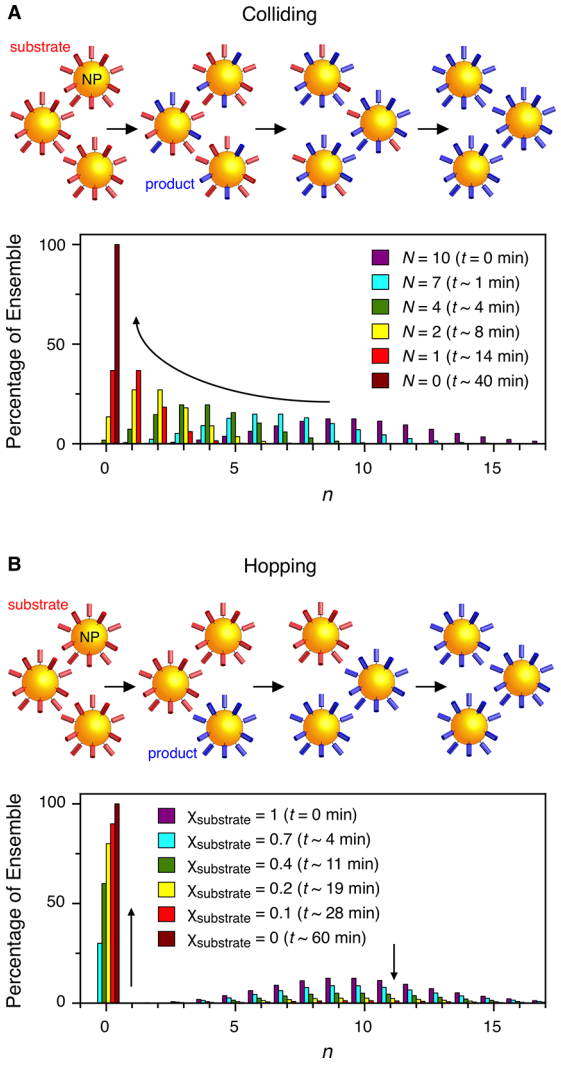

Figure 7. Illustrations of the progressive enzymatic turnover of NP-[substrate]$_N$ conjugates according to the (A) colliding model and (B) hopping model. For each model, cartoon snapshots are shown for the (sub)populations of NP-substrate/product conjugates at multiple time points in the reaction as well as the Poisson distribution(s) of the number of substrates per individual NP, n, for the average values, N. The reaction time listed for each value of N corresponds to the hypothetical progress curves in Figure 8.

initially obtained as the QD and dye PL emission intensities versus time. The dye/QD PL intensity ratio versus time is calculated from this data and also plotted. The data is modeled to be ideal with respect to FRET theory and free of noise, drift, and the nonspecific adsorption of product. Consequently, the progress curves for QD PL intensity versus time and the PL ratio versus time will both yield equivalent results from a full analysis, albeit the latter is thought to be a more robust metric for real experiments. To parametrize the thought experiment, we adopt an initial QD-[substrate–dye]$_N$ conjugate with a FRET efficiency of E = 0.75 at N = 10.

First, we consider a colliding model. The calibration for this model is a series of samples of QD-[substrate]$_N$ conjugates ranging from N = 0 to 10. Figure 8B shows the model calibration data. The trend for the QD PL intensity versus N is a hyperbolic function typical of FRET, and the trend for the dye/QD PL ratio is linear. The mock data assumes equal quantum yields for the QD and dye, but the trend in the PL ratio would be linear

DOI: 10.1021/acs.langmuir.8b02733
Langmuir XXXX, XXX, XXX–XXX

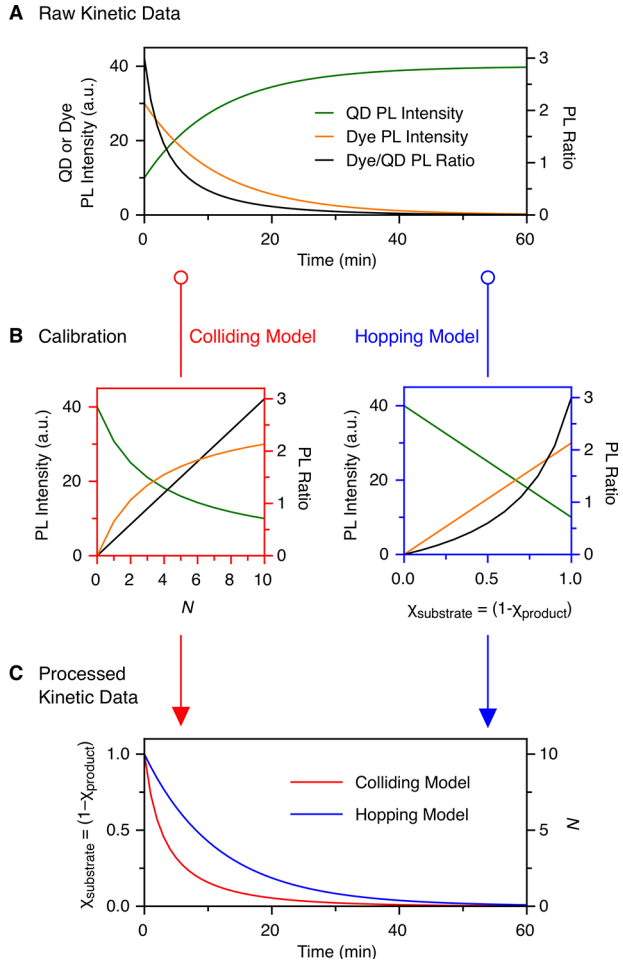

Figure 8. Thought experiment illustrating two different quantitative results for the same raw FRET assay data: (A) raw data measured as QD and dye PL intensity and their ratio versus time; (B) calibration data for the assumption of colliding and hopping models; and (C) resulting progress curves. Details of the derivation of the data can be found in the SI.

regardless of the ratio of quantum yields. The calibration data in Figure 8B converts the raw data to the stoichiometric progress curve in Figure 8C. The vertical axis of the progress curves in Figure 8C includes scales for the ensemble average number of peptides per QD, N, which is the logical metric for the colliding model, and for the mole fraction of substrate, calculated as $\chi_{substrate} = N/10$ for comparison to the hopping model.

The calibration for a hopping model is a series of samples with a mixture of QD-$[substrate]_{10}$ and QD-$[substrate]_0$ conjugates, with no intermediate values of N, where $\chi_{substrate}$ is the mole fraction of $N = 10$ conjugates. (In real experiments, QD-$[product]_{10}$ conjugates would be preferred over QD-$[substrate]_0$ conjugates to account for nonspecific adsorption.) The trend in the QD PL intensity is linear as a function of $\chi_{substrate}$, and the trend in the PL ratio is hyperbolic. The hopping model calibration data in Figure 8B converts the raw data to the stoichiometric progress curve in Figure 8C. Note that the progress curves for the hopping and colliding models are not superimposed. Rather, the assumption of a colliding model translates into an apparent faster rate of turnover. The difference arises from the requisite differences in calibration for the hopping and colliding models. The N and χ parameters are indeed comparable between the models because each corresponds to the same number of freely diffusing, hydrolyzed-product peptide fragments (despite representing a different makeup of the NP-substrate conjugates). A quirk is that the final progress curves for the two models become more similar as the FRET efficiency in the initial conjugate decreases and as nonspecific adsorption increases. Full details on the analysis of this thought experiment can be found in the SI.

Of course, there are prospective models that lie between the extremes of hopping and colliding. The degree to which the real enzymatic turnover of NP-$[substrate]_N$ conjugates approximates hopping or colliding may depend on the size of the NP and the value of N. Moreover, if we define pseudohopping as the turnover of a large number of substrates per NP per encounter with enzyme and define pseudocolliding as the turnover of a small number of substrates per NP per encounter with enzyme, then we must consider the possibilities of each of these models in isolation and as a mixed model that transitions from pseudohopping to pseudocolliding as the reaction progresses. Although the mathematics for these models can be devised, experiments must first establish and parametrize the model that is most appropriate. It is for this reason that we have recently stepped back from assigning a model to our data for the purposes of extracting apparent values of K_m and k_{cat}. Semiquantitative analysis remains possible without the selection of a colliding, hopping, or other model by comparing the nonstoichiometric progress curves with the QD PL intensity or PL ratio plotted versus time.[122,133] The caveat is that the properties of interest of

Table 1. Overview of Cited Studies on the Turnover of NP-Substrate Conjugates by Enzyme

material	surface chemistry[a]	substrate(s)	enzyme(s)	method(s)[b]	acceleration[c]	ref
Au NP	**1**, DNA	RNA	RNase H	FQ	1.8×−2.7×	122
QD	**12c**	peptide	trypsin	FRET	2.8×−4.7×	115
QD	**6**, **7**, **8**, **9**	peptide	trypsin	FRET and gels	12×−65×	55
			thrombin		1.5×−80×	
QD	**10**	PEG_3-Gly-Tyr	tyrosinase	CTQ	2.3×−3.2×	126
QD	**11**	peptide	collagenase, elastase	FRET	<1×	143
QD	**11**, **12a**−**f**	peptide	trypsin	FRET and simulation	3×−35×	79
QD	**8**, **9**, **10**, **12c**	peptide	trypsin	FRET and gels	3.5×−9×	133
			thrombin		<1×−5.6×	
			plasmin		3.6×−5.8×	

[a]The numbers refer to the structures in Figure 3. [b]FQ, fluorescence quenching. CTQ, charge-transfer quenching. [c]Factor by which the turnover of the NP-$[substrate]_N$ conjugate is faster than an equivalent amount of substrate without NP (values >1× indicate acceleration; values <1× indicate inhibition).

DOI: 10.1021/acs.langmuir.8b02733
Langmuir XXXX, XXX, XXX−XXX

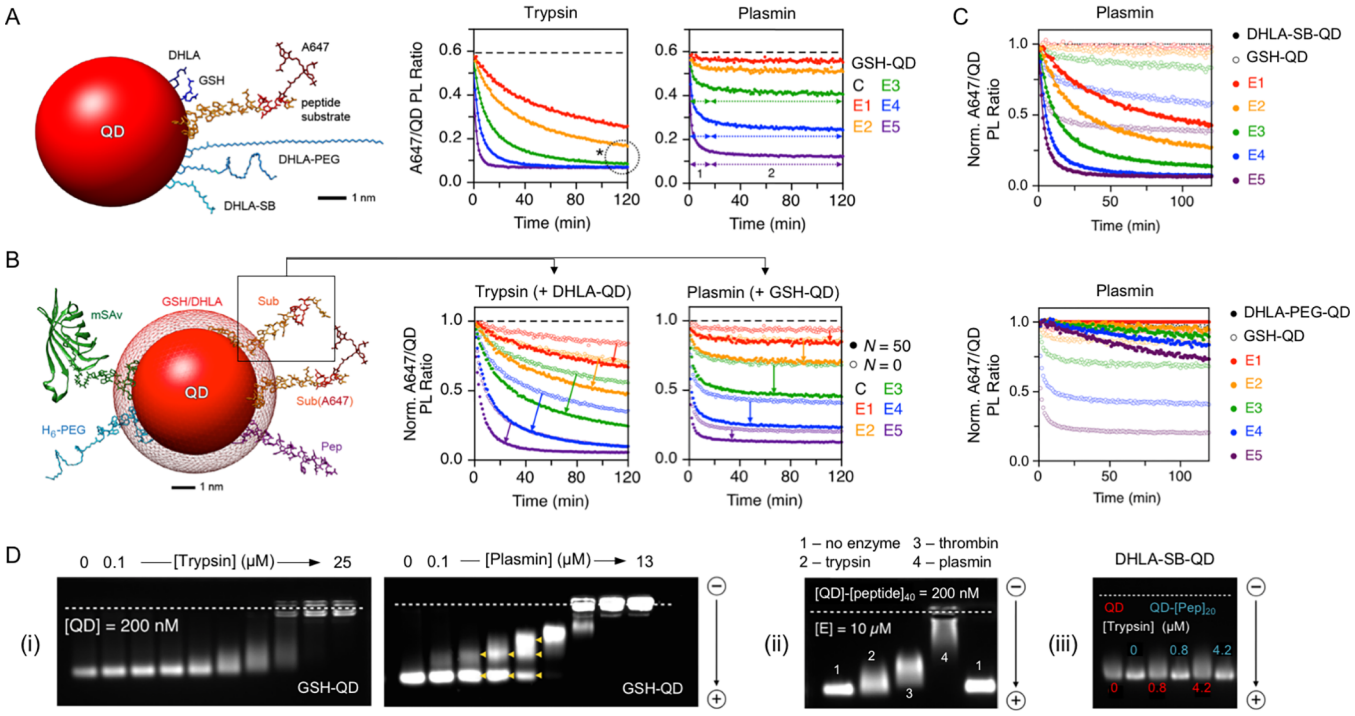

Figure 9. Protease adsorption affects the turnover of multivalent QD-peptide substrate conjugates. (A) Simplified cartoon of the conjugates with dye-labeled peptide substrates for a FRET assay and four different surface ligands. Representative progress curves for the turnover of the GSH-QD-[peptide substrate]$_{10}$ conjugates by trypsin and plasmin. (E1−E5 are different concentrations of enzyme, and C is a control without enzyme.) Trypsin shows one-phase/convergent progress curves; plasmin shows two-phase/nonconvergent progress curves. The asterisk (*) highlights convergence. (B) Simplified cartoon of the conjugates (ligands represented as a mesh shell) with added biomacromolecules and a dye-labeled peptide substrate, Sub(A647). Representative progress curves for X-QD-[Sub(A647)]$_{10}$-[Sub]$_N$. The progress curves show an enhancement in the rate or extent of substrate turnover. (C) Comparison of progress curves with plasmin for X-QD-[peptide substrate]$_{10}$ conjugates with X = GSH versus DHLA-SB and DHLA-PEG. DHLA-SB and DHLA-PEG convert the progress curves from two-phase/nonconvergent with GSH to one-phase/convergent. (D) Agarose gels illustrating the correlation between protease adsorption and kinetics: (i) comparison of trypsin (weaker) and plasmin (stronger) adsorption on GSH-QD; (ii) DHLA-QD-[peptide]$_{40}$ conjugates have lower adsorption than QD only (cf. panel i); and (iii) low adsorption of trypsin on DHLA-SB-QD and DHLA-SB-QD-[peptide]$_{20}$ conjugates. Adapted from ref 133. Copyright 2017 American Chemical Society.

the conjugate must be varied without substantially changing the FRET efficiency of the initial conjugate, for example, by using a fixed amount of the dye-labeled substrate and varying only the surface ligands or identity and number of additional unlabeled substrates or nonsubstrate biomolecules.[133] In real systems, the FRET efficiency generally changes slightly as the system changes, so small differences in progress curves must be interpreted cautiously. Nevertheless, much can still be learned about how changes in surface chemistry and other properties impact the turnover of NP-substrate conjugates.

■ ENZYME ACTIVITY AND INTERACTIONS WITH NPS

Overview. The previous sections of this article introduced concepts of enzymatic activity and interactions with NP-substrate conjugates apart from actual examples of experimental studies. We now add more substance to the discussion through a review of recent studies that address this research question. Table 1 summarizes several fundamental studies of the enzyme-catalyzed turnover of NP-substrate conjugates. (We apologize to the authors of any studies that we have inadvertently overlooked.) The results of these studies are distilled into prevailing factors that affect the rate of NP-substrate conjugate turnover, each with its own subsection. The final subsections address the recurring observation that the multivalent conjugation of substrate to a NP appears to accelerate enzyme activity and assess the current state of the hypothesis that a hopping model accounts for this acceleration.

Adsorption. A pair of studies that we have completed indicate an important role for the adsorption of enzyme on a NP in determining the kinetics of substrate turnover.[55,133] The proteases trypsin, thrombin, and plasmin were used as model enzymes, and glutathione (GSH, **9** in Figure 3), cysteine (**7**), 3-mercaptopropionic acid (MPA, **6**), dihydrolipoic acid (DHLA, **8**), DHLA-PEG (**12**), and DHLA-sulfobetaine (DHLA-SB, **10**) were used as surface ligands to functionalize CdSeS/ZnS and CdSe/CdS/ZnS QDs. The cumulative results of these studies can be summarized through five key experiments, as described below.

First, different surface ligand−protease pairings yielded different rates of turnover for X-QD-[peptide substrate]$_N$ conjugates and different shapes of progress curves, where X was one of the cysteine, DHLA, GSH, or MPA surface ligands and the proteases were trypsin and thrombin.[55] The progress curves were measured via FRET with a distal dye label on the peptide substrate. There was a general correlation between faster turnover and progress curves that were one-phase and convergent to a common end point for different protease concentrations, and between slower turnover and progress curves that were two-phase and nonconvergent for different protease concentrations. Trypsin exhibited one-phase/convergent progress curves regardless of X, whereas thrombin exhibited two-phase/nonconvergent progress curves. Even with the different shapes of the progress curve, the same qualitative trend in the rate of substrate turnover with X was

DOI: 10.1021/acs.langmuir.8b02733
Langmuir XXXX, XXX, XXX−XXX

observed with both trypsin and thrombin. Subsequent experiments, shown in part in Figure 9A, also revealed two-phase/nonconvergent progress curves for plasmin with X = DHLA and GSH.[133] The interpretation of the two-phase/nonconvergent progress curves was that thrombin or plasmin rapidly associated with X-QD-[peptide substrate]$_N$ conjugates, leading to an initial phase of efficient substrate hydrolysis that then transitioned to a second phase where the strong adsorption of protease on X-QD hindered diffusion to a new conjugate, causing a marked decrease in the ensemble rate of hydrolysis. Accordingly, the interpretation of the one-phase/convergent progress curves was that, to a first approximation, trypsin was free to diffuse from conjugate to conjugate because of weak (if any) adsorption on the X-QD.

A second set of experiments investigated the effect of X_2-QD on progress curves when mixed with X_1-QD-[substrate]$_N$ conjugates, where X_1 and X_2 are two different ligands.[55] The added X_2-QD had the strongest inhibitory effect with the X_2 = MPA and DHLA ligand coatings that were associated with the slowest turnover of substrate on CdSeS/ZnS QDs by thrombin and trypsin. In turn, the X_2 = GSH and cysteine ligand coatings that were associated with faster turnover had the smallest inhibitory effect. Thrombin was much more sensitive to X_2-QD than was trypsin, with the latter exhibiting almost no response to X_2-QD with X_2 = GSH and cysteine. These trends were fully consistent with expectations from the first set of experiments, further supporting the potential effect of the QD interface as an inhibitor of protease activity, putatively via strong adsorption and the loss of diffusion between conjugates.[55]

Two additional experiments further addressed surface effects, this time from the standpoint of surface passivation to reduce protease adsorption.[133] Figure 9B shows an example in which loading of the QD with an increasing number, *M*, of other biomacromolecules yielded an overall trend of increasing rate (one-phase progress curves) or extent (two-phase progress curves) of the substrate turnover. These conjugates were of the form X-QD-[peptide substrate]$_N$-[Y]$_M$, where Y was an additional substrate peptide, nonsubstrate peptide, protein, or discrete PEG molecules. The trend applied to trypsin, thrombin, and plasmin, albeit that the biggest effects were observed with plasmin, consistent with it being most prone to adsorption. In addition, it was found that a change from X = DHLA or GSH to X = DHLA-SB or DHLA-PEG resulted in a concomitant change from two-phase/nonconvergent progress curves to one-phase/convergent progress curves for plasmin activity. This result, shown in Figure 9C, was consistent with the well-characterized ability of PEG and zwitterionic coatings on NPs to resist nonspecific protein adsorption.[14−16] Overall, the two experiments demonstrated that the tuning of surface chemistry can mitigate inhibitory adsorption and recover protease activity.

The fifth and final set of experiments was runs of agarose gel electrophoresis, which linked all of the foregoing inferences of adsorption from progress curves to its direct observation.[55,133] Examples of gels are shown in Figure 9D. The adsorption of protease on QDs was observed in several ways: band streaking, band mobility shifts, the formation of multiple discrete bands of different mobility, and a complete loss of mobility. The order of these observations approximately trended with increasing affinity between the QD interface and protein (i.e., lower K_d) and less dynamic interactions (i.e., slower exchange between adsorbed and unbound states). Importantly, the gel-derived trends in protease adsorption on the QDs correlated with trends in progress curves and substrate turnover between surface ligands, X, between the three proteases, and with increased surface passivation from added biomacromolecules, Y. The caveat was that the protease concentrations at which adsorption was observed on a gel were higher than the concentrations used to measure progress curves, but there was a correlation in trends nonetheless.

A study by Díaz et al. drew conclusions similar to the above.[143] The activities of elastase and collagenase toward CdSe/CdZnS/ZnS QDs functionalized with a zwitterionic ligand (DHLA-CL4) and conjugated dye-labeled peptide substrate were compared. FRET was again used to measure progress curves. Differences between the progress curves for elastase and collagenase, albeit less than the differences we observed between plasmin and thrombin, were attributed to a much greater tendency for collagenase to adsorb on the QDs, which was likewise observed as mobility shifts for the QDs in agarose gel electrophoresis. Greater passivation of the QDs through conjugation of a greater number of substrate peptides also increased the rate of substrate turnover.[143]

The overarching conclusion from the above is that the minimization of enzyme adsorption on a NP is likely to maximize the rate of substrate turnover. That said, it remains an open question as to whether carefully optimized weak and dynamic adsorption can be more favorable than the complete and total elimination of adsorption. For example, in cases where steric hindrance (vide infra) is equal between different surface ligands on a QD, Díaz et al. have suggested that a weak affinity between a protease and NP may increase the residence time of the protease at the NP, potentially facilitating the turnover of conjugated substrate.[79] The affinity between RNase and Au NP-oligonucleotide conjugates has also been reported to accelerate nuclease activity.[122] The means by which weak adsorption might accelerate enzyme activity are discussed later.

Steric Hindrance. In one of our studies,[133] we saw a putative effect of steric hindrance between X = DHLA-SB and DHLA-PEG for X-QD-[peptide substrate]$_N$ conjugates. Although both ligands engendered one-phase/convergent progress curves with plasmin (cf. two-phase/nonconvergent progress curves with X = GSH, DHLA), a much slower rate of substrate turnover was observed for DHLA-PEG. Both the DHLA-SB and DHLA-PEG coatings resisted adsorption, so the difference in rate was attributed to the much larger size of the DHLA-PEG ligand. A significant portion of the length of the substrate was within the PEG layer around the QD, representing a potential hindrance for binding by plasmin.

The above conclusion was in agreement with a contemporary study by Díaz et al. that assessed the turnover of X-QD-[peptide substrate]$_N$ conjugates by trypsin, where X was a series of DHLA-PEG-R ligands (Figure 3C, **12**) and R was a variable functional group at the distal terminus of the PEG chain: amine, acetyl, methoxy, hydroxyl, carboxyl, or a zwitterionic group (denoted as CL4).[79] A DHLA-CL4 ligand without PEG was also evaluated as a control. Substrate turnover was fastest on the DHLA-CL4-QDs, consistent with steric hindrance from the PEG chains limiting access to the peptide substrate by trypsin. Moreover, atomistic molecular dynamics simulations suggested that there was some correlation between the solvent-accessible surface area (SASA) and turnover rates between the DHLA-PEG-R ligands, indicating an important role for steric hindrance in determining rates of substrate turnover. Figure 10 presents simple models of the sterically unhindered DHLA-CL4-QD-[peptide substrate]$_N$ conjugate and the hindered DHLA-PEG-OMe-QD-[peptide substrate]$_N$ conjugate as well as outputs of

DOI: 10.1021/acs.langmuir.8b02733
Langmuir XXXX, XXX, XXX−XXX

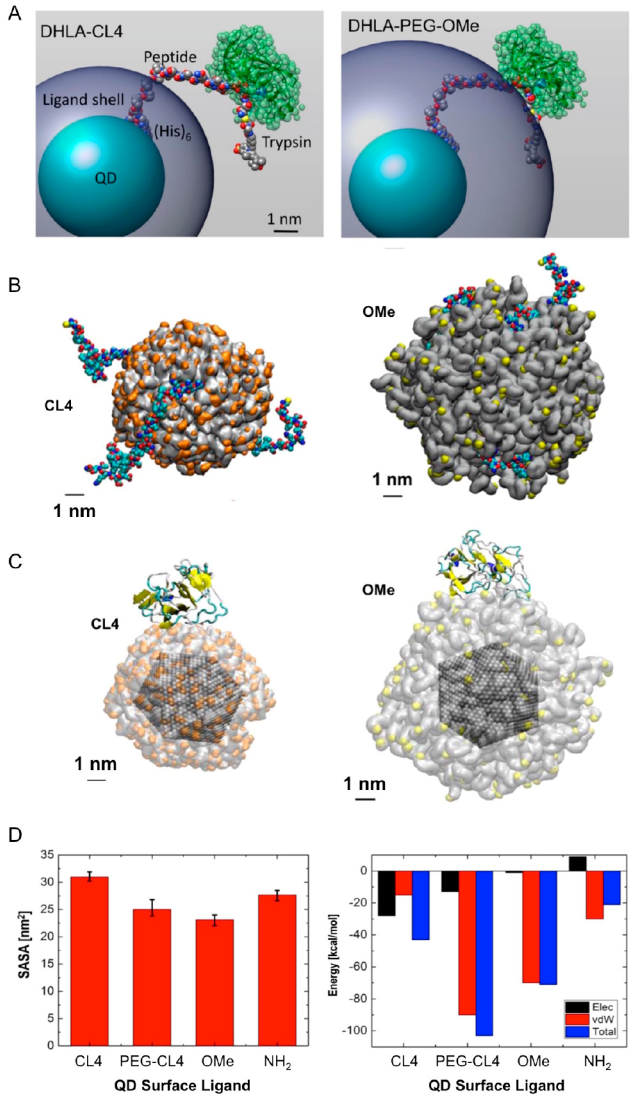

Figure 10. Illustration of steric versus adsorption effects for the turnover of X-QD-[peptide substrate]$_{7-12}$ conjugates for X = DHLA-CL4 and X = DHLA-PEG-OMe (abbreviated as CL4 and OMe). (A) Simple models of the conjugates. (B) Simulation results for the determination of solvent-accessible surface area (SASA) for the CL4 and OMe ligands. (C) Simulation results for the adsorption of trypsin on the same surface chemistries. (D) Plots of SASA and interaction energy (corresponding to panels B and C, respectively) for four different ligands: DHLA-CL4, DHLA-PEG-CL4, DHLA-PEG-OMe, and DHLA-PEG-NH_2. Sterics appeared to be the primary determinant of kinetics, with adsorption playing a secondary role. Adapted from ref 79. Copyright 2017 American Chemical Society.

the molecular dynamics simulations for SASA and adsorption energies (vide supra).

Interestingly, the observation of steric hindrance with QD-[substrate]$_N$ conjugates has, to date, been limited to effects from ligands. With compact ligands on QDs, large numbers of peptide per QD have not yet been reported to hinder protease activity versus smaller numbers. The likely explanation is that maximum peptide valences have been ≤60 per QD, whereas ligand numbers per QD have been estimated to be >200 per QD.[79] Higher densities of ligands are thus a likely factor; however, differences in the overall NP solvation for PEG ligands versus compact ligands and/or a higher affinity of proteases for peptides versus PEG cannot be ruled out. Co-assembly of peptide substrates with globular proteins also did not introduce detectable steric hindrance,[133] although there is not yet sufficient data to generalize this result.

In contrast to the above with QDs, there is some indication that peptides can be conjugated to Au NPs with sufficient density to cause steric hindrance, although these results are also not yet generalizable. A study by Yeh et al. found that chymotrypsin-catalyzed hydrolysis rates improved by 5-fold when the length of a peptide substrate conjugated to Au NPs increased from 9 residues to 13 residues, moving the cleavage sites further from the surface of the NP.[144] An additional 100-fold improvement was observed when the five inserted residues were converted from neutral to anionic. One explanation for this marked improvement, proposed by Yeh et al., was that the five anionic residues interacted favorably with the halo of cationic residues around the active site of chymotrypsin. Other possible explanations are that repulsion between neighboring poly-anionic peptides (and potentially residual citrate ligands on the Au NP) caused the peptides to be conjugated at a lower density and/or adopt a conformation that was more upright relative to the Au NP surface, alleviating steric hindrance. Moreover, the Au NPs modified with 9-mer and neutral 13-mer peptides had poor colloidal stability and required 0.1% bovine serum albumin (BSA) in solution as a stabilizer, whereas the Au NP modified with the anionic 13-mer probe did not.[144] BSA-stabilized aggregates of the former two NP materials or BSA adsorbed onto individual Au NPs are potential steric hindrances for chymotrypsin, and BSA is a potential competitive inhibitor as a second substrate. The initial 5-fold improvement with the neutral 13-mer peptide therefore seems attributable to a steric effect, but the subsequent 100-fold enhancement with the anionic 13-mer peptide is perhaps ambiguous or more complex in its origin. Nevertheless, the nature of peptide binding to Au NPs versus QDs, which is monothiol-gold binding displacing citrate functionalization versus hexahistidine-ZnS shell binding with a concomitant dithiol ligand, is such that a higher density of conjugated peptides should be achievable with Au NPs. Steric effects from substrate density are therefore more likely to occur with Au NPs.

Another example of steric hindrance with Au NPs was observed in assays for the activity of botulinum A light chain (BoLcA) protease activity.[145] The Au NPs were conjugated with peptide substrates, and turnover was compared between Au NPs with average diameters of 1.4, 6, and 18 nm. The turnover with the 6 and 18 nm Au NPs was 80-fold less than with 1.4 nm Au NPs. In analogous experiments with trypsin, the turnover was also less with the larger Au NPs but only 18-fold less versus the 1.4 nm Au NP. These different sensitivities to the steric effect of the NP was attributed to the larger size of BoLcA, which was double the molecular weight of trypsin, as well as its 2.4-nm-deep active site cleft.[145] Presumptive steric effects have also been observed with BoLcA and QD-peptide conjugates.[146]

Despite the above examples, steric hindrance is not a foregone conclusion with a high density of substrate on Au NPs. Prigodich et al. found that the high density of DNA oligonucleotides around a NP actually enhanced nuclease binding by a factor of about 2,[121,122] suggesting that there was either no steric hindrance or that it was overwhelmed by the effect of enhanced affinity (e.g., high local concentration).

Interfacial Environment. Many enzymes have a pH, temperature, and other parameters that optimize their activity. As noted earlier, the environment at the NP interface is different than the environment of bulk solution, so this local environment

DOI: 10.1021/acs.langmuir.8b02733
Langmuir XXXX, XXX, XXX−XXX

may influence enzymatic activity toward a NP-substrate conjugate. One such example, shown in Figure 11, arises with

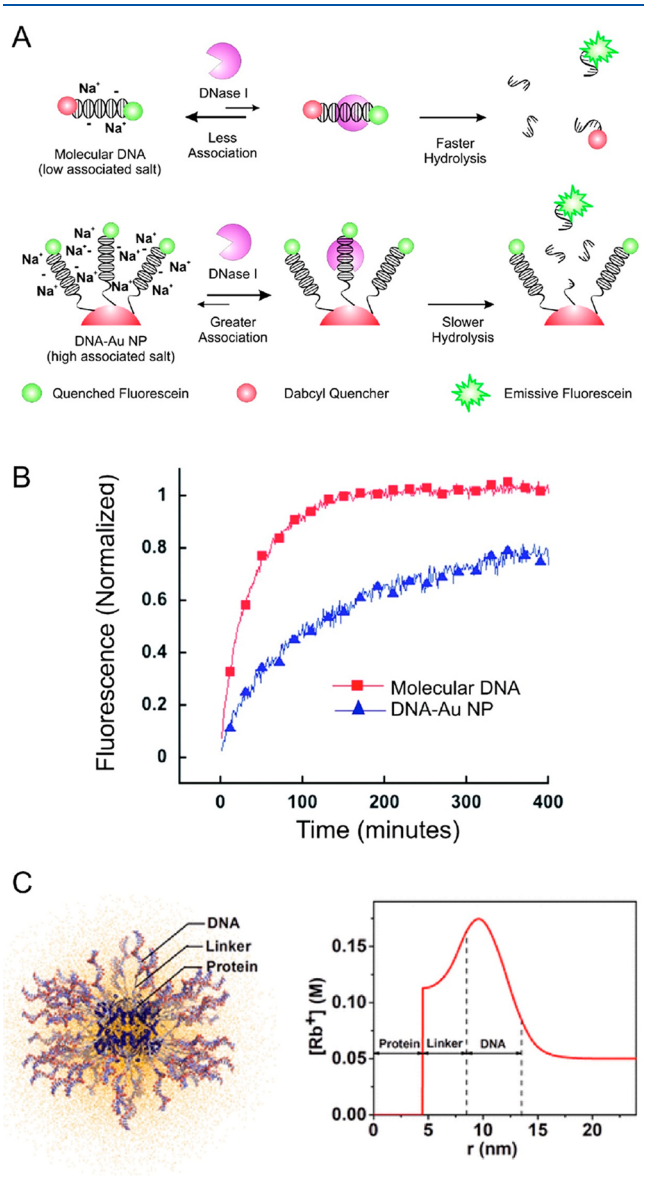

Figure 11. Impact of monovalent cation concentration in the interfacial environment of a multivalent NP-oligonucleotide conjugate on nuclease activity. (A) Although DNase I has a higher affinity for a Au NP-DNA conjugate versus an isolated oligonucleotide, the rate of hydrolysis is slower. (B) Progress curves for the assays illustrated in panel A. Panels A and B are reproduced from ref 121. Copyright 2009 American Chemical Society. (C) Schematic of a protein-spherical nucleic acid conjugate (left) and radial profile of monovalent cation concentration from the center of the protein. A similar profile is expected for Au NP-[oligonucleotide]$_N$ conjugates. Reproduced from ref 147. Copyright 2018 American Chemical Society.

spherical nucleic acids, which are densely multivalent Au NP-DNA oligonucleotide conjugates. Compared to DNA alone, these materials are ca. 4-fold more resistant to hydrolysis by DNase I because the high local concentration of monovalent cations at the NP interface inhibits nuclease activity by displacing divalent cation cofactors from the enzyme.[121] This high concentration of cations arises from countering the polyanionic character of the oligonucleotides and from a local influx of anions from osmotic pressure that must be balanced by additional cations.[147] The inhibitory effect decreases with lower negative charge density on the Au NP and for nucleases that are engineered to be more tolerant of salt.[121]

Although relatively few studies have (so far) uncovered an effect of the local NP environment on enzyme activity toward substrate-on-NP configurations, possibilities can be extrapolated from the converse enzyme-on-NP configurations because the substrate−enzyme interaction occurs at the interface between the NP and bulk solution in both cases. For example, Breger et al. found that phosphotriesterase activity was enhanced versus bulk solution when conjugated to a QD, concluding that different solvation at the NP interface increased the rate of product dissociation from the enzyme, which was known to be slower than the rate of hydrolysis and thus limiting.[130] Another study postulated that an enhancement in the activity of lipase adsorbed to Au NPs was from the interface lowering the activation energy barrier for the formation of the enzyme−substrate complex.[129]

A caution is that alterations of enzyme activity from the local environment at the NP interface are not necessarily straightforward to distinguish from an allosteric or similar effect induced by contact with the NP or other conjugated biomacromolecules. This concept is more intuitive for enzyme-on-NP configurations but may also be applicable to some NP-substrate conjugates. Experiments that correlate enzyme activity with changes induced in the NP interfacial environment by upstream changes in bulk solution are thus important supporting evidence.

Acceleration of Substrate Turnover. The studies cited above have shown that many factors can affect enzyme activity toward NP-substrate conjugates. A feature common to several of these and other studies is an acceleration of substrate turnover with NP-substrate conjugates versus equivalent quantities of enzyme and substrate in bulk solution without NP. Examples include trypsin, thrombin, and plasmin activity toward QD-[peptide]$_N$ substrates,[55,79,133] RNase H activity toward Au NP-[oligonucleotide]$_N$ conjugates,[122] and tyrosinase activity toward QD-[tyrosine]$_N$ conjugates.[126] The accelerations have been an approximate doubling of turnover rates at the low end and between 1 to 2 orders of magnitude at the high end, with each example listed in Table 1. However, the acceleration of activity is not universal. It has already been mentioned that the local environment of a Au NP-oligonucleotide conjugate can inhibit some nucleases,[121] and one study found that DHLA-CL4-QD-[peptide substrate]$_N$ conjugates inhibited the activity of collagenase and elastase,[143] although the same nominal materials accelerated trypsin activity 35-fold in another study.[79] We have also seen indications that batch-to-batch variation can yield acceleration or inhibition for nominally similar materials.[148] These examples do not necessarily challenge the concept of enzymatic acceleration with NP-[substrate]$_N$ conjugates, but once again highlight the complexity of the systems.

Collision theory for reaction rates is a useful framework for analyzing the acceleration of enzymatic activity toward NP-[substrate]$_N$ conjugates because, irrespective of a hopping or colliding model, a change in the kinetics rather than the thermodynamics of substrate to product conversion is expected. To begin, consider an x μM concentration of the NP-[substrate]$_N$ conjugate versus an Nx μM concentration of only substrate, both mixed with E nM of enzyme. The latter scenario has a greater frequency of collisions if the concepts of collision cross-section and productive orientation are momentarily neglected. The NP must therefore increase both of the latter parameters by a combined factor of greater than N if there is to

DOI: 10.1021/acs.langmuir.8b02733
Langmuir XXXX, XXX, XXX−XXX

be an acceleration of substrate turnover. Starting with the collision cross-section, the physical size of a NP is typically much greater than that of a substrate alone and is made larger by multivalent conjugation of a substrate. For example, a typical QD-[peptide]$_N$ conjugate has a QD in the range of 1.5−4 nm in radius, and FRET data suggests that peptides extend the radius by an additional 2 to 3 nm.[149,150] The collision cross-section is clearly much larger for the NP-[substrate]$_N$ conjugate than for an individual substrate molecule, as depicted in Figure 12A. A

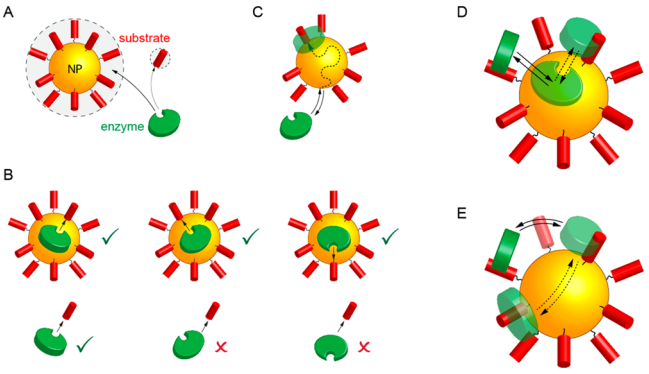

Figure 12. Illustrations of the potential mechanisms through which the turnover of a substrate is made more efficient by multivalent conjugation to a NP. (A) The NP-[substrate]$_N$ conjugate has a larger collisional cross-section versus discrete substrate molecules. (B) The close proximity between multiple substrates increases the likelihood of a collision with a productive orientation of enzyme. (C) The enzyme collides with the NP and diffuses along its surface to find the substrate. (D) Reversible adsorption to the NP surface facilitates enzyme reassociation with substrate after dissociation. (E) The close proximity between multiple substrates facilitates enzyme reassociation with substrate after dissociation. The importance of each of these mechanisms is likely to depend on the details of the conjugate.

rough estimate is between 3-fold and 25-fold larger for the example of a QD-[peptide]$_N$ conjugate. The Stokes−Einstein equation also indicates that the cross-section for a NP should increase at a faster rate than its diffusion coefficient decreases as the NP diameter increases.

It is also expected that the likelihood of a productive collision is higher with a NP-[substrate]$_N$ conjugate. First, at the moment of an initial collision, the NP conjugate will display multiple substrates in close proximity with different orientations relative to the enzyme. This situation is expected to increase the probability of a productive mutual orientation between enzyme and substrate, as depicted in Figure 12B. Second, transient interactions or migration along a NP surface, or temporary capture within the hydration shell of the NP-substrate conjugate (an effect reported with other nanoscale enzymatic systems[151]), illustrated in Figure 12C, have the potential to increase the residence time of the enzyme at the NP, giving it more opportunity to rotate into a productive orientation and bind to a substrate molecule. These factors also increase the likelihood that the enzyme will reassociate with a new substrate molecule after dissociation from another, as depicted in Figure 12D, as does the high local concentration of substrate with larger N, depicted in Figure 12E. These overall concepts inspire the hypothesis that sufficiently weak but nonzero adsorption or another interaction with the NP-[substrate]$_N$ conjugate may lead to an enhancement of turnover, even though moderate or strong adsorption is inhibitory.

A question that arises is if any of the above modifications to the parameters of collision theory represent a real change in the intrinsic K_m and k_{cat} for an enzyme−substrate combination. The answer depends somewhat on perspective, and we will use the case of a QD-[peptide]$_N$ conjugate to illustrate. If each peptide molecule is to be a unique substrate, then the presumption is that there is no enhancement in either K_m or k_{cat} and that a good model must account for the features of the multivalent NP configuration that lead to acceleration (and perhaps even tolerate unfavorable changes in K_m and k_{cat} from loss of degrees of freedom or steric effects). However, if the entire conjugate is to be treated as the substrate, then the acceleration of turnover is reconciled with new values of K_m and k_{cat}, preferably labeled as *apparent* values because of the different molecular-scale processes versus the conventional Michaelis−Menten model. For example, many of the processes depicted in Figure 12 suggest that the apparent value of the Michaelis constant, $K_{m,\,app}$, would, at minimum, be a convolution of the conventional enzyme−substrate K_m and the adsorption constant, K_{ads}, for the enzyme on the NP. We reserve judgment on which perspective is most practical until a hopping, colliding, or corresponding pseudomodel of turnover is confirmed.

In sum, multivalent NP-substrate conjugates have the potential to yield large accelerations of enzyme activity because of the high local concentration of substrate at their interface, but strong adsorption and steric hindrance reduce or negate the acceleration, and further nuances remain to be determined.

Evidence for a Hopping Model. Much of how to conceptualize and analyze the enzymatic turnover of NP-substrate conjugates seems to hinge on the confirmation of a model for how it occurs, whether hopping or otherwise. The ideas of a high local concentration of substrate at the NP interface and weak affinity interactions between the enzyme and NP-substrate conjugate, discussed in the previous subsection, are the crux of the rationale for a hopping model of activity. For many readers, a hopping or pseudohopping model of enzymatic turnover will seem intuitive for NP-[substrate]$_N$ conjugates; however, to our knowledge, there has yet to be a direct observation of two discrete populations of NP-[substrate]$_N$ and NP-[product]$_N$ that shrink and grow concurrently as the enzymatic reaction progresses. Rather, evidence has been indirect, as discussed below.

One of the most compelling bits of evidence is the observation that the complete turnover of QD-[peptide]$_N$ conjugates by proteases requires an equal or shorter amount of time as N increases, with N reaching values as high as 60.[115,133,143] Analogous results have been observed for increasing N with Au NP-[oligonucleotide]$_N$ conjugates and turnover by nucleases.[121,122] If only one or a small number of substrates were turned over in each encounter, as in colliding and pseudocolliding models, then larger N should require more encounters between enzyme and NP and therefore a longer time for the reaction to reach completion. In contrast, a hopping or pseudohopping model predicts these experimental results. A potential counterargument posits that larger N progressively increases the probability of productive encounters and thus offsets the need for more encounters in a colliding or pseudocolliding model; however, some observations are not consistent with this hypothesis. The mobility shifts for QD-[peptide]$_N$ conjugates observed by agarose gel electrophoresis diminish and become negligible as N increases, such that the effective size of the conjugates approximately saturates well before the maximum loading of peptide per QD is reached,[133] so

DOI: 10.1021/acs.langmuir.8b02733
Langmuir XXXX, XXX, XXX−XXX

a putative larger size cannot account for the steady or increasing rate of turnover as N continues to increase. Moreover, when N was kept constant while the density of substrates in Au NP-$[\text{oligonucleotide}]_N$ conjugates was decreased by increasing the effective linker length between the substrate and Au NP, the rate of turnover by nuclease decreased despite the larger size of the conjugate.[122] The overall results of the above studies suggest that more substrate per NP increases the frequency with which intersubstrate hopping occurs, as per Figure 12E.

Other evidence comes from the previously noted real and predicted adsorption or association of enzyme with NP-$[\text{substrate}]_N$ conjugates. Excess components of a NP-$[\text{substrate}]_N$ conjugate in bulk solution can also act as competitive inhibitors, as observed for certain surface chemistries of QD mixed with QD-$[\text{peptide}]_N$ conjugates and protease,[55] and with ssDNA mixed with Au NP-$[\text{DNA/RNA}]_N$-$[\text{ssDNA}]_M$ conjugates and RNase H.[122] These results suggest that the processes in Figure 12C−E can occur, as can an analog of the process in Figure 12E, between inequivalent biomacromolecules. Presumably, the energetics of these processes can be tuned to be either a contribution to the overall acceleration of enzyme activity or a deceleration that competes with other accelerating processes in Figure 12. Although preliminary, this idea is supported by the aforementioned observation by Díaz et al. that there was secondary correlation between observed turnover rates and the calculated interaction energies between QDs and trypsin.[79]

Certainly, a hopping mechanism is not unequivocal at this point and should not be taken as fact; however, the results to date point in this direction, and the odds for a hopping or pseudohopping model appear to be better than for a colliding or pseudocolliding model for some types of multivalent NP-substrate conjugates.

PERSPECTIVE AND CONCLUSIONS

The importance of enzymes as current and future biomarkers and drug targets is undeniable, and NPs of many kinds have both well-established and still-developing benefits for biological detection and targeting. Knowing more about how enzymes interact with NPs will enable further advancement and innovation with respect to these application areas. More fundamental research is needed and must address the complexity of the NP interface and the limitations of current tools for elucidating its structure and properties.

So what is required to better understand the enzymatic turnover of NP-substrate conjugates?

One answer is more holistic studies. Taking our work as an example, we have utilized ensemble FRET assays and gel electrophoresis supplemented by comparisons to kinetic models of enzyme activity and simple structural models of enzymes.[55,115,133,148] These methods have been insightful but homogenized the NP-enzyme systems and only scratched the surface of their overall complexity. We have also made efforts to confirm that there is a qualitative persistence of trends across multiple batches of NPs but have only been able to attribute quantitative differences in these trends to undetermined heterogeneity and batch-to-batch variation. Determining the root causes of batch-to-batch variation and more general differences in behavior between various NP materials and methods of preparation will require an analysis that is both multifaceted and detailed:

- Physical characterization of inorganic NPs, including their distributions of hard size, hydrodynamic size, zeta potential, and other structural or morphological properties (e.g., via TEM, DLS, SAXS);
- Chemical characterization of the inorganic and organic components of functionalized NPs (e.g., via FTIR, NMR, ICP-MS/OES, XPS, EDX);
- Kinetic models that are tailored to a putative model of turnover for a NP-substrate conjugate, with clear definitions of parameters, assumptions, and limitations;
- Structural models of enzymes, including basic models with the mapping of surface charges and hydrophobicity, as well as more advanced models based on molecular dynamics, energy minimization, and other simulations;
- Broad scope and other steps to establish generality; for example, experiments with multiple NP materials (e.g., different composition or size), various preparations and functionalizations (e.g., series of different surface ligands), replicate batches of the same nominal NP, and multiple substrates and/or multiple enzymes.

Well-executed holistic studies are undoubtedly a substantial but worthwhile undertaking for developing a detailed understanding of enzymatic activity toward NP-substrate conjugates. Aside from establishing the generality of results, a broader scope of experiments will help address domino effects and a hierarchy of trends. The term "domino effect" refers to a nominal change in one property that leads to changes in other properties. For example, a change in the number of macromolecular substrates per NP has the potential to change not only the local concentration of substrate but also the average conformation of those substrates and the steric hindrance for enzyme−NP and enzyme−substrate interactions. Other potential examples arise from the aforementioned propagation of changes from one layer of chemistry to another in the NP-substrate conjugate: a change in the NP material alters the density of surface ligands, or a change in the identity of the surface ligand alters the average conformation of a substrate. A hierarchy of trends will be useful for parsing domino effects by reliably predicting which of several possible effects is most important. For example, steric hindrance may predominate differences in enzyme activity between two NP-substrate conjugates with surface ligands of very different molecular weight, whereas the relative affinity of the enzyme toward the NP may predominate if the surface ligands have similar molecular weight. The ambition is that it will be possible to use a small number of discrete factors to predict behavior even if the real systems are influenced by a complex continuum of factors.

Another answer to the question of how to better understand the enzymatic turnover of NP-substrate conjugates is to shift away from ensemble methods and toward single-particle measurements. These measurements avoid the ensemble averaging that homogenizes a heterogeneous system and are anticipated to reveal mechanistic details essential to the modeling of kinetics, including the determination of a hopping, colliding, or pseudomodel of turnover. Any distinct subpopulations of NPs within an ensemble will also be revealed. A second useful approach will be separation methods that divide a heterogeneous ensemble of NPs into semihomogeneous fractions for enzymatic assays. A comparison of progress curves or other data for these fractions versus the ensemble, in combination with a knowledge of the property by which the NPs were fractionated, will provide insight into correlations between NP properties and enzymatic activity. In the same vein, high-throughput and automated methods for the preparation of

DOI: 10.1021/acs.langmuir.8b02733
Langmuir XXXX, XXX, XXX−XXX

libraries of NP-substrate conjugates and for assays of enzymatic activity toward these conjugates will enable machine learning methods for elucidating how various properties affect enzymatic activity. Machine learning methods have, for example, already been used for applications in organic synthesis,[152−154] materials development,[155,156] prediction of protein−ligand binding,[157] and determination of the substrate specificity of enzymes.[158]

An expanded role for computational modeling and simulation is also warranted. There is the potential for this role to go beyond energy minimization and molecular dynamics modeling of enzyme−NP interactions at a homogenized interface and instead address heterogeneity at individual facets, between subpopulations of NPs in an ensemble, and between NP identities. These interactions can then be further extrapolated to simulate substrate turnover and ultimately produce a theoretical progress curve for an ensemble that can be matched to experimental data. Inference of mechanistic details then becomes possible through iterative tweaks of the parameters of the models until matched to experiments. Moreover, simulation is perhaps the best available method of extracting facet-dependent behaviors with NPs. These behaviors are potentially important, as has recently come to light with bulk interfacial systems with tethered biomolecules.[159]

A detailed understanding of enzymatic activity toward NP-substrate conjugates leads to another question: what benefits will come from this fundamental knowledge?

In the context of in vitro molecular diagnostics, more sensitive and more rapid assays of enzyme biomarkers are possible with a NP-substrate conjugate that optimizes and accelerates enzyme activity and concurrently resists or slows fouling with a protein corona in biological fluid. Such a material has substantial value for point-of-care applications in particular.

Another useful lens through which to view this question is the control that in vivo biological systems exert over enzyme activity toward substrates, mirrored against the comparatively poor substrate specificity when the same enzymes are used in vitro. With a detailed understanding of NP−enzyme and substrate−enzyme interactions, there is the potential for the rational design of a synthetic conjugate that achieves some of the in vivo substrate specificity of an enzyme: for example, a substrate optimized for the active site of an enzyme (e.g., amino acid sequence for a protease) in combination with surface chemistry on the NP that interacts either favorably with the target enzyme or unfavorably with nontarget enzymes of similar substrate specificity. Our observation that the functionalization of a QD surface with MPA ligands can virtually shut down thrombin activity but retain trypsin activity is an illustration of this general concept,[55] albeit not suitable for biomedical application. We also have recent results that show that it is possible to rationally functionalize a NP to accelerate target enzyme activity rather than decelerate nontarget enzyme activity.[148] This behavior arose from cofunctionalizing a QD with a substrate for thrombin and peptide fragments of a receptor that allosterically interacted with thrombin to enhance its activity, although it was still strongly dependent on QD surface chemistry. Facet-dependent functionalization and interactions with enzymes, coupled with the synthesis of anisotropic NPs such as plates and rods, may prove to be yet another route to generating selectivity. Overall, enhanced specificity will benefit in vitro assays and cellular and in vivo imaging probes for fundamental biological research and clinical application.

A better understanding of enzymatic activity toward NPs also benefits enzyme-mediated drug delivery and theranostics.[160,161] Here, the concept is that a substrate tethers a drug or prodrug payload to a NP for release via enzymatic activity at the site of disease. Although organic NPs such as liposomes and polymer materials predominate NP-mediated drug delivery,[162,163] inorganic NPs are also of interest and stand to enable chemotherapy in combination with other therapies; for example, Au NPs and iron oxide NPs have prospective application in photothermal and magnetic hyperthermia therapies, respectively.[164−167] In addition, magnetic NPs and lanthanide NPs are also of interest as contrast agents for imaging.[168,169] Current QD materials are of little interest for clinical drug delivery but are nonetheless promising as model NP vectors for fundamental research on drug delivery.[170] With aberrant enzyme activity as a hallmark of many diseases (e.g., kinases and proteases in cancers and neurodegenerative disease[171−175]), the control of enzymatic activity toward NP-substrate conjugates represents a possible means of controlling the location and rate of drug delivery. Moreover, there is also the possibility of using NPs as a scaffold for enzyme inhibitors (as many drugs are), analogous to what has been discussed at length for the NP as a scaffold for enzyme substrates. The high local concentration of inhibitor (or drug) at the NP interface may increase potency, particularly when combined with NP surface chemistry that is tailored to be very favorable and, ideally, somewhat selective for adsorption of the target enzyme.

To conclude, the activity of enzymes toward NP-substrate conjugates is an interesting and important avenue of research. A full understanding of such systems represents a complex and nuanced problem to solve but will enable important advances in biomedical research and development and will be another step toward clinical applications of NPs. Success in solving this problem will require a concerted effort that leverages a large variety of tools for colloid and interface science, with several potential rewards to reap.

■ ASSOCIATED CONTENT

Supporting Information

The Supporting Information is available free of charge on the ACS Publications website at DOI: 10.1021/acs.langmuir.8b02733.

Table of ligands from Figure 3, calculation of local concentration, additional discussion of substrate design and properties, and calculations for the colliding versus hopping thought experiment (PDF)

■ AUTHOR INFORMATION

Corresponding Author

*E-mail: algar@chem.ubc.ca.

ORCID

W. Russ Algar: 0000-0003-3442-7072
William J. Peveler: 0000-0002-9829-2683

Notes

The authors declare no competing financial interest.

DOI: 10.1021/acs.langmuir.8b02733
Langmuir XXXX, XXX, XXX−XXX

Biographies

W. Russ Algar received his Ph.D. degree in chemistry (2010) from the University of Toronto under the supervision of Prof. Ulrich Krull and then undertook postdoctoral work at the Center for Bio/Molecular Science and Engineering, U.S. Naval Research Laboratory, with Dr. Igor L. Medintz. In 2012, he joined the Department of Chemistry at the University of British Columbia, where he is now an associate professor. His current research is at the interface of analytical, physical, biological, and materials chemistry and focuses on the development, characterization, and applications of luminescent materials in bioanalysis.

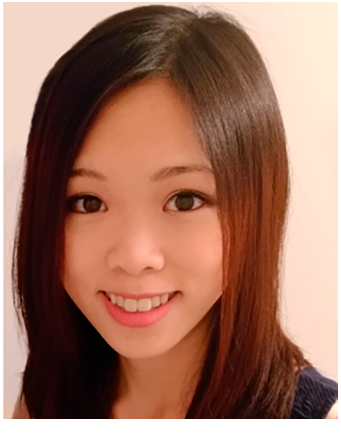

Tiffany Jeen completed her M.Sc. degree (2018) at the University of British Columbia under the supervision of Prof. W. Russ Algar. Her research focused on the surface functionalization of quantum dots to help further develop these materials as tools for bioanalysis.

Melissa Massey is a postdoctoral researcher with Prof. W. Russ Algar in the Department of Chemistry at the University of British Columbia. She received her Ph.D. in chemistry (2011) from the University of Toronto under the supervision of Prof. Ulrich Krull. Her current research focuses on the use of luminescent lanthanide complexes and quantum dots for FRET-based bioanalytical applications.

William J. Peveler completed his M.Chem. at the University of Oxford and received his Ph.D. (2015) from UCL on the topic of arrays for explosives detection. He then undertook postdoctoral work with Profs. William Rosenberg and Claire Carmalt at UCL and Prof. Vincent Rotello at the University of Massachusetts, Amherst, developing a sensor array for liver disease. Most recently, he was awarded a Killam Postdoctoral Research Fellowship to undertake a year of study at the University of British Columbia, with Prof. W. Russ Algar, before returning to the U.K. to take up an independent LKAS Fellowship at the University of Glasgow. His current research interests are the synthesis of new molecular and nanoscale materials for biomarker sensing, with a focus on liver disease and near-patient testing.

Jérémie Asselin is a postdoctoral researcher with Prof. W. Russ Algar in the Department of Chemistry at the University of British Columbia. He received his Ph.D. in chemistry (2018) at Université Laval under the supervision of Prof. Denis Boudreau. His current research interests include the synthesis of composite nanoarchitectures, the characterization of materials by ensemble and single-particle optical techniques, and the development of fluorescence-based analytical biosensors.

■ ACKNOWLEDGMENTS

The authors thank the Office of Naval Research (program manager: L. Kienker), the Natural Sciences and Engineering Research Council of Canada (NSERC), the Canada Foundation for Innovation (CFI), the British Columbia Knowledge Development Fund, and the University of British Columbia for support of their research program. W.R.A. gratefully acknowledges a Canada Research Chair (Tier 2), a Michael Smith Foundation for Health Research Scholar Award, and an Alfred P. Sloan Fellowship. T.J. gratefully acknowledges support from the NSERC CREATE NanoMat program. W.J.P. gratefully

DOI: 10.1021/acs.langmuir.8b02733
Langmuir XXXX, XXX, XXX−XXX

acknowledges the Izaak Walton Killam Memorial Fund for a postdoctoral research fellowship and the University of Glasgow for a Lord Kelvin Adam Smith Fellowship.

REFERENCES

(1) Sapsford, K. E.; Algar, W. R.; Berti, L.; Gemmill, K. B.; Casey, B. J.; Oh, E.; Stewart, M. H.; Medintz, I. L. Functionalizing Nanoparticles with Biological Molecules: Developing Chemistries That Facilitate Nanotechnology. *Chem. Rev.* **2013**, *113*, 1904−2074.
(2) Zhou, W.; Gao, X.; Liu, D. B.; Chen, X. Y. Gold Nanoparticles for in Vitro Diagnostics. *Chem. Rev.* **2015**, *115*, 10575−10636.
(3) Wegner, K. D.; Hildebrandt, N. Quantum Dots: Bright and Versatile in Vitro and in Vivo Fluorescence Imaging Biosensors. *Chem. Soc. Rev.* **2015**, *44*, 4792−4834.
(4) Wu, L. H.; Mendoza-Garcia, A.; Li, Q.; Sun, S. H. Organic Phase Syntheses of Magnetic Nanoparticles and Their Applications. *Chem. Rev.* **2016**, *116*, 10473−10512.
(5) Dreaden, E. C.; Alkilany, A. M.; Huang, X. H.; Murphy, C. J.; El-Sayed, M. A. The Golden Age: Gold Nanoparticles for Biomedicine. *Chem. Soc. Rev.* **2012**, *41*, 2740−2779.
(6) Sperling, R. A.; Parak, W. J. Surface Modification, Functionalization and Bioconjugation of Colloidal Inorganic Nanoparticles. *Philos. Trans. R. Soc., A* **2010**, *368*, 1333−1383.
(7) Boles, M. A.; Ling, D.; Hyeon, T.; Talapin, D. V. The Surface Science of Nanocrystals. *Nat. Mater.* **2016**, *15*, 141−153.
(8) Walkey, C. D.; Chan, W. C. W. Understanding and Controlling the Interaction of Nanomaterials with Proteins in a Physiological Environment. *Chem. Soc. Rev.* **2012**, *41*, 2780−2799.
(9) Lynch, I.; Dawson, K. A. Protein-Nanoparticle Interactions. *Nano Today* **2008**, *3*, 40−47.
(10) Pelaz, B.; Charron, G.; Pfeiffer, C.; Zhao, Y. L.; de la Fuente, J. M.; Liang, X. J.; Parak, W. J.; del Pino, P. Interfacing Engineered Nanoparticles with Biological Systems: Anticipating Adverse Nanobio Interactions. *Small* **2013**, *9*, 1573−1584.
(11) Park, S.; Hamad-Schifferli, K. Nanoscale Interfaces to Biology. *Curr. Opin. Chem. Biol.* **2010**, *14*, 616−622.
(12) Pulido-Reyes, G.; Leganes, F.; Fernandez-Pinas, F.; Rosal, R. Bio-Nano Interface and Environment: A Critical Review. *Environ. Toxicol. Chem.* **2017**, *36*, 3181−3193.
(13) Li, Y. C.; Xu, Y. L.; Fleischer, C. C.; Huang, J.; Lin, R.; Yang, L.; Mao, H. Impact of Anti-Biofouling Surface Coatings on the Properties of Nanomaterials and Their Biomedical Applications. *J. Mater. Chem. B* **2018**, *6*, 9−24.
(14) Khutoryanskiy, V. V. Beyond PEGylation: Alternative Surface-Modification of Nanoparticles with Mucus-Inert Biomaterials. *Adv. Drug Delivery Rev.* **2018**, *124*, 140−149.
(15) Cao, Z. Q.; Jiang, S. Y. Super-Hydrophilic Zwitterionic Poly(Carboxybetaine) and Amphiphilic Non-Ionic Poly(Ethylene Glycol) for Stealth Nanoparticles. *Nano Today* **2012**, *7*, 404−413.
(16) Garcia, K. P.; Zarschler, K.; Barbaro, L.; Barreto, J. A.; O'Malley, W.; Spiccia, L.; Stephan, H.; Graham, B. Zwitterionic-Coated "Stealth" Nanoparticles for Biomedical Applications: Recent Advances in Countering Biomolecular Corona Formation and Uptake by the Mononuclear Phagocyte System. *Small* **2014**, *10*, 2516−2529.
(17) Carrillo-Carrion, C.; Carril, M.; Parak, W. J. Techniques for the Experimental Investigation of the Protein Corona. *Curr. Opin. Biotechnol.* **2017**, *46*, 106−113.
(18) Caracciolo, G.; Farokhzad, O. C.; Mahmoudi, M. Biological Identity of Nanoparticles in Vivo: Clinical Implications of the Protein Corona. *Trends Biotechnol.* **2017**, *35*, 257−264.
(19) Bilensoy, E. Cationic Nanoparticles for Cancer Therapy. *Expert Opin. Drug Delivery* **2010**, *7*, 795−809.
(20) Wang, Z. Y.; Liu, G.; Zheng, H. R.; Chen, X. Y. Rigid Nanoparticle-Based Delivery of Anti-Cancer siRNA: Challenges and Opportunities. *Biotechnol. Adv.* **2014**, *32*, 831−843.
(21) Copeland, R. A. Why Enzymes as Drug Targets? In *Evaluation of Enzyme Inhibitors in Drug Discovery*; Copeland, R. A., Ed.; John Wiley & Sons: 2013.
(22) Tegl, G.; Schiffer, D.; Sigl, E.; Heinzle, A.; Guebitz, G. M. Biomarkers for Infection: Enzymes, Microbes, and Metabolites. *Appl. Microbiol. Biotechnol.* **2015**, *99*, 4595−4614.
(23) Borgono, C. A.; Diamandis, E. P. The Emerging Roles of Human Tissue Kallikreins in Cancer. *Nat. Rev. Cancer* **2004**, *4*, 876−890.
(24) Roy, R.; Yang, J.; Moses, M. A. Matrix Metalloproteinases as Novel Biomarkers and Potential Therapeutic Targets in Human Cancer. *J. Clin. Oncol.* **2009**, *27*, 5287−5297.
(25) Mease, R. C.; Foss, C. A.; Pomper, M. G. PET Imaging in Prostate Cancer: Focus on Prostate-Specific Membrane Antigen. *Curr. Top. Med. Chem.* **2013**, *13*, 951−962.
(26) Ong, I. L. H.; Yang, K. L. Recent Developments in Protease Activity Assays and Sensors. *Analyst* **2017**, *142*, 1867−1881.
(27) Kim, Y. P.; Kim, H. S. Nanoparticles for Use in Enzyme Assays. *ChemBioChem* **2016**, *17*, 275−282.
(28) Xin, Y. R.; Yin, M. M.; Zhao, L. Y.; Meng, F. L.; Luo, L. Recent Progress on Nanoparticle-Based Drug Delivery Systems for Cancer Therapy. *Cancer Biol. Med.* **2017**, *14*, 228−241.
(29) Hu, Q.; Katti, P. S.; Gu, Z. Enzyme-Responsive Nanomaterials for Controlled Drug Delivery. *Nanoscale* **2014**, *6*, 12273−12286.
(30) Vranish, J. N.; Ancona, M. G.; Walper, S. A.; Medintz, I. L. Pursuing the Promise of Enzymatic Enhancement with Nanoparticle Assemblies. *Langmuir* **2018**, *34*, 2901−2925.
(31) Johnson, B. J.; Algar, W. R.; Malanoski, A. P.; Ancona, M. G.; Medintz, I. L. Understanding Enzymatic Acceleration at Nanoparticle Interfaces: Approaches and Challenges. *Nano Today* **2014**, *9*, 102−131.
(32) Ding, S. W.; Cargill, A. A.; Medintz, I. L.; Claussen, J. C. Increasing the Activity of Immobilized Enzymes with Nanoparticle Conjugation. *Curr. Opin. Biotechnol.* **2015**, *34*, 242−250.
(33) Misson, M.; Zhang, H.; Jin, B. Nanobiocatalyst Advancements and Bioprocessing Applications. *J. R. Soc., Interface* **2015**, *12*, 20140891.
(34) Ansari, S. A.; Husain, Q. Potential Applications of Enzymes Immobilized on/in Nano Materials: A Review. *Biotechnol. Adv.* **2012**, *30*, 512−523.
(35) Koshland, D. E. The Key-Lock Theory and the Induced Fit Theory. *Angew. Chem., Int. Ed. Engl.* **1995**, *33*, 2375−2378.
(36) Hedstrom, L. Serine Protease Mechanism and Specificity. *Chem. Rev.* **2002**, *102*, 4501−4523.
(37) Ma, W. Z.; Tang, C.; Lai, L. H. Specificity of Trypsin and Chymotrypsin: Loop-Motion-Controlled Dynamic Correlation as a Determinant. *Biophys. J.* **2005**, *89*, 1183−1193.
(38) Pravda, L.; Berka, K.; Varekova, R. S.; Sehnal, D.; Banas, P.; Laskowski, R. A.; Koca, J.; Otyepka, M. Anatomy of Enzyme Channels. *BMC Bioinf.* **2014**, *15*, 379.
(39) Sanders, C. R.; Hutchison, J. M. Membrane Properties That Shape the Evolution of Membrane Enzymes. *Curr. Opin. Struct. Biol.* **2018**, *51*, 80−91.
(40) Marianayagam, N. J.; Sunde, M.; Matthews, J. M. The Power of Two: Protein Dimerization in Biology. *Trends Biochem. Sci.* **2004**, *29*, 618−625.
(41) Hardy, J. A.; Wells, J. A. Searching for New Allosteric Sites in Enzymes. *Curr. Opin. Struct. Biol.* **2004**, *14*, 706−715.
(42) Krishnaswamy, S. Exosite-Driven Substrate Specificity and Function in Coagulation. *J. Thromb. Haemostasis* **2005**, *3*, 54−67.
(43) Huntington, J. A. Molecular Recognition Mechanisms of Thrombin. *J. Thromb. Haemostasis* **2005**, *3*, 1861−1872.
(44) Castellino, F. J.; Ploplis, V. A. Structure and Function of the Plasminogen/Plasmin System. *Thromb. Haemostasis* **2005**, *93*, 647−654.
(45) Huntington, J. A. How Na^+ Activates Thrombin - a Review of the Functional and Structural Data. *Biol. Chem.* **2008**, *389*, 1025−1035.
(46) Chahal, G.; Thorpe, M.; Hellman, L. The Importance of Exosite Interactions for Substrate Cleavage by Human Thrombin. *PLoS One* **2015**, *10*, e0129511.
(47) Russo Krauss, I.; Pica, A.; Merlino, A.; Mazzarella, L.; Sica, F. Duplex-Quadruplex Motifs in a Peculiar Structural Organization Cooperatively Contribute to Thrombin Binding of a DNA Aptamer. *Acta Crystallogr., Sect. D: Biol. Crystallogr.* **2013**, *69*, 2403−2411.

DOI: 10.1021/acs.langmuir.8b02733
Langmuir XXXX, XXX, XXX−XXX

(48) Law, R. H. P.; Caradoc-Davies, T.; Cowieson, N.; Horvath, A. J.; Quek, A. J.; Encarnacao, J. A.; Steer, D.; Cowan, A.; Zhang, Q.; Lu, B. G. C.; et al. The X-Ray Crystal Structure of Full-Length Human Plasminogen. *Cell Rep.* **2012**, *1*, 185−190.
(49) Razeto, A.; Galunsky, B.; Kasche, V.; Wilson, K. S.; Lamzin, V. S. High Resolution Structure of Bovine Alpha-Chymotrypsin. *RSCB Protein Data Bank* **2006**, DOI: 10.2210/pdb1YPH/pdb.
(50) Garcia-Granda, S.; Chamorro Gavilanes, J. A. Native Bovine Pancreatic Trypsin. *RSCB Protein Data Bank*; 2005.
(51) Gandhi, P. S.; Chen, Z. W.; Appelbaum, E.; Zapata, F.; Di Cera, E. Structural Basis of Thrombin-Protease-Activated Receptor Interactions. *IUBMB Life* **2011**, *63*, 375−382.
(52) Lane, D. A.; Philippou, H.; Huntington, J. A. Directing Thrombin. *Blood* **2005**, *106*, 2605−2612.
(53) Ponting, C. P.; Marshall, J. M.; Cederholm-Williams, S. A. Plasminogen - a Structural Review. *Blood Coagulation Fibrinolysis* **1992**, *3*, 605−614.
(54) Shemetov, A. A.; Nabiev, I.; Sukhanova, A. Molecular Interaction of Proteins and Peptides with Nanoparticles. *ACS Nano* **2012**, *6*, 4585−4602.
(55) Wu, M.; Algar, W. R. Acceleration of Proteolytic Activity Associated with Selection of Thiol Ligand Coatings on Quantum Dots. *ACS Appl. Mater. Interfaces* **2015**, *7*, 2535−2545.
(56) Kotov, N. A. Inorganic Nanoparticles as Protein Mimics. *Science* **2010**, *330*, 188−189.
(57) Gentleman, D. J.; Chan, W. C. W. A Systematic Nomenclature for Codifying Engineered Nanostructures. *Small* **2009**, *5*, 426−431.
(58) Lim, S. J.; Ma, L.; Schleife, A.; Smith, A. M. Quantum Dot Surface Engineering: Toward Inert Fluorophores with Compact Size and Bright, Stable Emission. *Coord. Chem. Rev.* **2016**, *320-321*, 216−237.
(59) Barnard, A. S.; Chen, Y. Kinetic Modelling of the Shape-Dependent Evolution of Faceted Gold Nanoparticles. *J. Mater. Chem.* **2011**, *21*, 12239−12245.
(60) Mori, T.; Hegmann, T. Determining the Composition of Gold Nanoparticles: A Compilation of Shapes, Sizes, and Calculations Using Geometric Considerations. *J. Nanopart. Res.* **2016**, *18*, 295.
(61) Carbo-Argibay, E.; Rodriguez-Gonzalez, B. Controlled Growth of Colloidal Gold Nanoparticles: Single-Crystalline Versus Multiply-Twinned Particles. *Isr. J. Chem.* **2016**, *56*, 214−226.
(62) You, C. C.; De, M.; Han, G.; Rotello, V. M. Tunable Inhibition and Denaturation of Alpha-Chymotrypsin with Amino Acid-Functionalized Gold Nanoparticles. *J. Am. Chem. Soc.* **2005**, *127*, 12873−12881.
(63) De, M.; Rana, S.; Akpinar, H.; Miranda, O. R.; Arvizo, R. R.; Bunz, U. H. F.; Rotello, V. M. Sensing of Proteins in Human Serum Using Conjugates of Nanoparticles and Green Fluorescent Protein. *Nat. Chem.* **2009**, *1*, 461−465.
(64) Mizuhara, T.; Saha, K.; Moyano, D. F.; Kim, C. S.; Yan, B.; Kim, Y. K.; Rotello, V. M. Acylsulfonamide-Functionalized Zwitterionic Gold Nanoparticles for Enhanced Cellular Uptake at Tumor pH. *Angew. Chem., Int. Ed.* **2015**, *54*, 6567−6570.
(65) Cutler, J. I.; Auyeung, E.; Mirkin, C. A. Spherical Nucleic Acids. *J. Am. Chem. Soc.* **2012**, *134*, 1376−1391.
(66) Pensa, E.; Cortes, E.; Corthey, G.; Carro, P.; Vericat, C.; Fonticelli, M. H.; Benitez, G.; Rubert, A. A.; Salvarezza, R. C. The Chemistry of the Sulfur-Gold Interface: In Search of a Unified Model. *Acc. Chem. Res.* **2012**, *45*, 1183−1192.
(67) Burgi, T. Properties of the Gold-Sulphur Interface: From Self-Assembled Monolayers to Clusters. *Nanoscale* **2015**, *7*, 15553−15567.
(68) Hu, G. X.; Jin, R. C.; Jiang, D. E. Beyond the Staple Motif: A New Order at the Thiolate-Gold Interface. *Nanoscale* **2016**, *8*, 20103−20110.
(69) Hakkinen, H. The Gold-Sulfur Interface at the Nanoscale. *Nat. Chem.* **2012**, *4*, 443−455.
(70) Vericat, C.; Vela, M. E.; Benitez, G.; Carro, P.; Salvarezza, R. C. Self-Assembled Monolayers of Thiols and Dithiols on Gold: New Challenges for a Well-Known System. *Chem. Soc. Rev.* **2010**, *39*, 1805−1834.
(71) Zeng, C. J.; Qian, H. F.; Li, T.; Li, G.; Rosi, N. L.; Yoon, B.; Barnett, R. N.; Whetten, R. L.; Landman, U.; Jin, R. C. Total Structure and Electronic Properties of the Gold Nanocrystal $Au_{36}(SR)_{24}$. *Angew. Chem., Int. Ed.* **2012**, *51*, 13114−13118.
(72) Grumelli, D.; Maza, F. L.; Kern, K.; Salvarezza, R. C.; Carro, P. Surface Structure and Chemistry of Alkanethiols on Au(100)-(1 × 1) Substrates. *J. Phys. Chem. C* **2016**, *120*, 291−296.
(73) Algar, W. R.; Susumu, K.; Delehanty, J. B.; Medintz, I. L. Semiconductor Quantum Dots in Bioanalysis: Crossing the Valley of Death. *Anal. Chem.* **2011**, *83*, 8826−8837.
(74) Uyeda, H. T.; Medintz, I. L.; Jaiswal, J. K.; Simon, S. M.; Mattoussi, H. Synthesis of Compact Multidentate Ligands to Prepare Stable Hydrophilic Quantum Dot Fluorophores. *J. Am. Chem. Soc.* **2005**, *127*, 3870−3878.
(75) Stewart, M. H.; Susumu, K.; Mei, B. C.; Medintz, I. L.; Delehanty, J. B.; Blanco-Canosa, J. B.; Dawson, P. E.; Mattoussi, H. Multidentate Poly(Ethylene Glycol) Ligands Provide Colloidal Stability to Semiconductor and Metallic Nanocrystals in Extreme Conditions. *J. Am. Chem. Soc.* **2010**, *132*, 9804−9813.
(76) Susumu, K.; Mei, B. C.; Mattoussi, H. Multifunctional Ligands Based on Dihydrolipoic Acid and Polyethylene Glycol to Promote Biocompatibility of Quantum Dots. *Nat. Protoc.* **2009**, *4*, 424−436.
(77) Mei, B. C.; Susumu, K.; Medintz, I. L.; Delehanty, J. B.; Mountziaris, T. J.; Mattoussi, H. Modular Poly(Ethylene Glycol) Ligands for Biocompatible Semiconductor and Gold Nanocrystals with Extended pH and Ionic Stability. *J. Mater. Chem.* **2008**, *18*, 4949−4958.
(78) Susumu, K.; Uyeda, H. T.; Medintz, I. L.; Pons, T.; Delehanty, J. B.; Mattoussi, H. Enhancing the Stability and Biological Functionalities of Quantum Dots Via Compact Multifunctional Ligands. *J. Am. Chem. Soc.* **2007**, *129*, 13987−13996.
(79) Díaz, S. A.; Seni, S.; Boeneman Gemmill, K.; Brown, C. W.; Oh, E.; Susumu, K.; Stewart, M. H.; Breger, J. C.; Aragonés, G. L.; Field, L. D.; et al. Elucidating Surface Ligand-Dependent Kinetic Enhancement of Proteolytic Activity at Surface-Modified Quantum Dots. *ACS Nano* **2017**, *11*, 5884−5896.
(80) Susumu, K.; Oh, E.; Delehanty, J. B.; Blanco-Canosa, J. B.; Johnson, B. J.; Jain, V.; Hervey, W. J.; Algar, W. R.; Boeneman, K.; Dawson, P. E.; et al. Multifunctional Compact Zwitterionic Ligands for Preparing Robust Biocompatible Semiconductor Quantum Dots and Gold Nanoparticles. *J. Am. Chem. Soc.* **2011**, *133*, 9480−9496.
(81) Park, J.; Nam, J.; Won, N.; Jin, H.; Jung, S.; Jung, S.; Cho, S.-H.; Kim, S. Compact and Stable Quantum Dots with Positive, Negative, or Zwitterionic Surface: Specific Cell Interactions and Non-Specific Adsorptions by the Surface Charges. *Adv. Funct. Mater.* **2011**, *21*, 1558−1566.
(82) Weeraman, C.; Yatawara, A. K.; Bordenyuk, A. N.; Benderskii, A. V. Effect of Nanoscale Geometry on Molecular Conformation: Vibrational Sum-Frequency Generation of Alkanethiols on Gold Nanoparticles. *J. Am. Chem. Soc.* **2006**, *128*, 14244−14245.
(83) Frederick, M. T.; Achtyl, J. L.; Knowles, K. E.; Weiss, E. A.; Geiger, F. M. Surface-Amplified Ligand Disorder in CdSe Quantum Dots Determined by Electron and Coherent Vibrational Spectroscopies. *J. Am. Chem. Soc.* **2011**, *133*, 7476−7481.
(84) McBride, J.; Treadway, J.; Feldman, L. C.; Pennycook, S. J.; Rosenthal, S. J. Structural Basis for near Unity Quantum Yield Core/Shell Nanostructures. *Nano Lett.* **2006**, *6*, 1496−1501.
(85) Smith, A. M.; Marbella, L. E.; Johnston, K. A.; Hartmann, M. J.; Crawford, S. E.; Kozycz, L. M.; Seferos, D. S.; Millstone, J. E. Quantitative Analysis of Thiolated Ligand Exchange on Gold Nanoparticles Monitored by ^{1}H NMR Spectroscopy. *Anal. Chem.* **2015**, *87*, 2771−2778.
(86) Knauf, R. R.; Lennox, J. C.; Dempsey, J. L. Quantifying Ligand Exchange Reactions at CdSe Nanocrystal Surfaces. *Chem. Mater.* **2016**, *28*, 4762−4770.
(87) Schrurs, F.; Lison, D. Join the Dialogue. *Nat. Nanotechnol.* **2012**, *7*, 545.
(88) Sapsford, K. E.; Tyner, K. M.; Dair, B. J.; Deschamps, J. R.; Medintz, I. L. Analyzing Nanomaterial Bioconjugates: A Review of Current and Emerging Purification and Characterization Techniques. *Anal. Chem.* **2011**, *83*, 4453−4488.

DOI: 10.1021/acs.langmuir.8b02733
Langmuir XXXX, XXX, XXX−XXX

(89) Xia, Y. N.; Xiong, Y. J.; Lim, B.; Skrabalak, S. E. Shape-Controlled Synthesis of Metal Nanocrystals: Simple Chemistry Meets Complex Physics? *Angew. Chem., Int. Ed.* **2009**, *48*, 60−103.
(90) Yin, Y.; Alivisatos, A. P. Colloidal Nanocrystal Synthesis and the Organic-Inorganic Interface. *Nature* **2005**, *437*, 664−670.
(91) Wang, F. D.; Tang, R.; Buhro, W. E. The Trouble with TOPO; Identification of Adventitious Impurities Beneficial to the Growth of Cadmium Selenide Quantum Dots, Rods, and Wires. *Nano Lett.* **2008**, *8*, 3521−3524.
(92) Zhuang, Z. B.; Peng, Q.; Li, Y. D. Controlled Synthesis of Semiconductor Nanostructures in the Liquid Phase. *Chem. Soc. Rev.* **2011**, *40*, 5492−5513.
(93) Grzelczak, M.; Perez-Juste, J.; Mulvaney, P.; Liz-Marzan, L. M. Shape Control in Gold Nanoparticle Synthesis. *Chem. Soc. Rev.* **2008**, *37*, 1783−1791.
(94) Lesnyak, V.; Gaponik, N.; Eychmuller, A. Colloidal Semiconductor Nanocrystals: The Aqueous Approach. *Chem. Soc. Rev.* **2013**, *42*, 2905−2929.
(95) Lee, S. F.; Osborne, M. A. Brightening, Blinking, Bluing and Bleaching in the Life of a Quantum Dot: Friend or Foe? *ChemPhysChem* **2009**, *10*, 2174−2191.
(96) Gorham, J. M.; Rohlfing, A. B.; Lippa, K. A.; MacCuspie, R. I.; Hemmati, A.; Holbrook, R. D. Storage Wars: How Citrate-Capped Silver Nanoparticle Suspensions Are Affected by Not-So-Trivial Decisions. *J. Nanopart. Res.* **2014**, *16*, 14.
(97) Aldana, J.; Lavelle, N.; Wang, Y. J.; Peng, X. G. Size-Dependent Dissociation pH of Thiolate Ligands from Cadmium Chalcogenide Nanocrystals. *J. Am. Chem. Soc.* **2005**, *127*, 2496−2504.
(98) Aldana, J.; Wang, Y. A.; Peng, X. G. Photochemical Instability of CdSe Nanocrystals Coated by Hydrophilic Thiols. *J. Am. Chem. Soc.* **2001**, *123*, 8844−8850.
(99) Richman, E. K.; Hutchison, J. E. The Nanomaterial Characterization Bottleneck. *ACS Nano* **2009**, *3*, 2441−2446.
(100) Nel, A. E.; Brinker, C. J.; Parak, W. J.; Zink, J. I.; Chan, W. C. W.; Pinkerton, K. E.; Xia, T.; Baer, D. R.; Hersam, M. C.; Weiss, P. S. Where Are We Heading in Nanotechnology Environmental Health and Safety and Materials Characterization? *ACS Nano* **2015**, *9*, 5627−5630.
(101) Murphy, C. J.; Buriak, J. M. Best Practices for the Reporting of Colloidal Inorganic Nanomaterials. *Chem. Mater.* **2015**, *27*, 4911−4913.
(102) Zobel, M.; Neder, R. B.; Kimber, S. A. J. Universal Solvent Restructuring Induced by Colloidal Nanoparticles. *Science* **2015**, *347*, 292−294.
(103) Jiang, S. Y.; Cao, Z. Q. Ultralow-Fouling, Functionalizable, and Hydrolyzable Zwitterionic Materials and Their Derivatives for Biological Applications. *Adv. Mater.* **2010**, *22*, 920−932.
(104) Chen, S. F.; Li, L. Y.; Zhao, C.; Zheng, J. Surface Hydration: Principles and Applications toward Low-Fouling/Nonfouling Biomaterials. *Polymer* **2010**, *51*, 5283−5293.
(105) Smith, A. M.; Lee, A. A.; Perkin, S. The Electrostatic Screening Length in Concentrated Electrolytes Increases with Concentration. *J. Phys. Chem. Lett.* **2016**, *7*, 2157−2163.
(106) Wang, D. W.; Nap, R. J.; Lagzi, I.; Kowalczyk, B.; Han, S. B.; Grzybowski, B. A.; Szleifer, I. How and Why Nanoparticle's Curvature Regulates the Apparent pK_a of the Coating Ligands. *J. Am. Chem. Soc.* **2011**, *133*, 2192−2197.
(107) Algar, W. R.; Krull, U. J. Characterization of the Adsorption of Oligonucleotides on Mercaptopropionic Acid-Coated CdSe/ZnS Quantum Dots Using Fluorescence Resonance Energy Transfer. *J. Colloid Interface Sci.* **2011**, *359*, 148−154.
(108) Conroy, E. M.; Li, J. J.; Kim, H.; Algar, W. R. Self-Quenching, Dimerization, and Homo-FRET in Hetero-FRET Assemblies with Quantum Dot Donors and Multiple Dye Acceptors. *J. Phys. Chem. C* **2016**, *120*, 17817−17828.
(109) Wiley, D. T.; Webster, P.; Gale, A.; Davis, M. E. Transcytosis and Brain Uptake of Transferrin-Containing Nanoparticles by Tuning Avidity to Transferrin Receptor. *Proc. Natl. Acad. Sci. U. S. A.* **2013**, *110*, 8662−8667.
(110) Parak, W. J.; Pellegrino, T.; Micheel, C. M.; Gerion, D.; Williams, S. C.; Alivisatos, A. P. Conformation of Oligonucleotides Attached to Gold Nanocrystals Probed by Gel Electrophoresis. *Nano Lett.* **2003**, *3*, 33−36.
(111) Colangelo, E.; Chen, Q. B.; Davidson, A. M.; Paramelle, D.; Sullivan, M. B.; Volk, M.; Levy, R. Computational and Experimental Investigation of the Structure of Peptide Monolayers on Gold Nanoparticles. *Langmuir* **2017**, *33*, 438−449.
(112) Hill, H. D.; Millstone, J. E.; Banholzer, M. J.; Mirkin, C. A. The Role Radius of Curvature Plays in Thiolated Oligonucleotide Loading on Gold Nanoparticles. *ACS Nano* **2009**, *3*, 418−424.
(113) Algar, W. R.; Kim, H.; Medintz, I. L.; Hildebrandt, N. Emerging Non-Traditional Forster Resonance Energy Transfer Configurations with Semiconductor Quantum Dots: Investigations and Applications. *Coord. Chem. Rev.* **2014**, *263-264*, 65−85.
(114) Medintz, I. L.; Clapp, A. R.; Brunel, F. M.; Tiefenbrunn, T.; Uyeda, H. T.; Chang, E. L.; Deschamps, J. R.; Dawson, P. E.; Mattoussi, H. Proteolytic Activity Monitored by Fluorescence Resonance Energy Transfer through Quantum-Dot-Peptide Conjugates. *Nat. Mater.* **2006**, *5*, 581−589.
(115) Algar, W. R.; Malonoski, A.; Deschamps, J. R.; Blanco-Canosa, J. B.; Susumu, K.; Stewart, M. H.; Johnson, B. J.; Dawson, P. E.; Medintz, I. L. Proteolytic Activity at Quantum Dot-Conjugates: Kinetic Analysis Reveals Enhanced Enzyme Activity and Localized Interfacial "Hopping". *Nano Lett.* **2012**, *12*, 3793−3802.
(116) Tang, A. M.; Mei, B.; Wang, W. J.; Hu, W. L.; Li, F.; Zhou, J.; Yang, Q.; Cui, H.; Wu, M.; Liang, G. L. FITC-Quencher Based Caspase 3-Activatable Nanoprobes for Effectively Sensing Caspase 3 in Vitro and in Cells. *Nanoscale* **2013**, *5*, 8963−8967.
(117) Huang, S.; Xiao, Q.; He, Z. K.; Liu, Y.; Tinnefeld, P.; Su, X. R.; Peng, X. N. A High Sensitive and Specific QDs FRET Bioprobe for MNase. *Chem. Commun.* **2008**, 5990−5992.
(118) Gill, R.; Willner, I.; Shweky, I.; Banin, U. Fluorescence Resonance Energy Transfer in CdSe/ZnS-DNA Conjugates: Probing Hybridization and DNA Cleavage. *J. Phys. Chem. B* **2005**, *109*, 23715−23719.
(119) Ray, P. C.; Fortner, A.; Darbha, G. K. Gold Nanoparticle Based FRET Assay for the Detection of DNA Cleavage. *J. Phys. Chem. B* **2006**, *110*, 20745−20748.
(120) Huang, Y.; Zhao, S. L.; Liang, H.; Chen, Z. F.; Liu, Y. M. Multiplex Detection of Endonucleases by Using a Multicolor Gold Nanobeacon. *Chem. - Eur. J.* **2011**, *17*, 7313−7319.
(121) Seferos, D. S.; Prigodich, A. E.; Giljohann, D. A.; Patel, P. C.; Mirkin, C. A. Polyvalent DNA Nanoparticle Conjugates Stabilize Nucleic Acids. *Nano Lett.* **2009**, *9*, 308−311.
(122) Prigodich, A. E.; Alhasan, A. H.; Mirkin, C. A. Selective Enhancement of Nucleases by Polyvalent DNA-Functionalized Gold Nanoparticles. *J. Am. Chem. Soc.* **2011**, *133*, 2120−2123.
(123) Freeman, R.; Finder, T.; Gill, R.; Willner, I. Probing Protein Kinase (CK2) and Alkaline Phosphatase with CdSe/ZnS Quantum Dots. *Nano Lett.* **2010**, *10*, 2192−2196.
(124) Ghadiali, J. E.; Cohen, B. E.; Stevens, M. M. Protein Kinase-Actuated Resonance Energy Transfer in Quantum Dot-Peptide Conjugates. *ACS Nano* **2010**, *4*, 4915−4919.
(125) Ghadiali, J. E.; Lowe, S. B.; Stevens, M. M. Quantum-Dot-Based FRET Detection of Histone Acetyltransferase Activity. *Angew. Chem., Int. Ed.* **2011**, *50*, 3417−3420.
(126) Zhu, X. L.; Hu, J.; Zhao, Z. H.; Sun, M. J.; Chi, X. Q.; Wang, X. M.; Gao, J. H. Kinetic and Sensitive Analysis of Tyrosinase Activity Using Electron Transfer Complexes: In Vitro and Intracellular Study. *Small* **2015**, *11*, 862−870.
(127) Goddard, J. P.; Reymond, J. L. Enzyme Assays for High-Throughput Screening. *Curr. Opin. Biotechnol.* **2004**, *15*, 314−322.
(128) Wysocki, L. M.; Lavis, L. D. Advances in the Chemistry of Small Molecule Fluorescent Probes. *Curr. Opin. Chem. Biol.* **2011**, *15*, 752−759.
(129) Wu, C.-S.; Wu, C.-T.; Yang, Y.-S.; Ko, F.-H. An Enzymatic Kinetics Investigation into the Significantly Enhanced Activity of

DOI: 10.1021/acs.langmuir.8b02733
Langmuir XXXX, XXX, XXX−XXX

Functionalized Gold Nanoparticles. *Chem. Commun.* **2008**, 5327−5329.
(130) Breger, J. C.; Ancona, M. G.; Walper, S. A.; Oh, E.; Susumu, K.; Stewart, M. H.; Deschamps, J. R.; Medintz, I. L. Understanding How Nanoparticle Attachment Enhances Phosphotriesterase Kinetic Efficiency. *ACS Nano* **2015**, *9*, 8491−8503.
(131) Brown, C. W., III; Oh, E.; Hastman, D. A.; Walper, S. A.; Susumu, K.; Stewart, M. H.; Deschamps, J. R.; Medintz, I. L. Kinetic Enhancement of the Diffusion-Limited Enzyme Beta-Galactosidase When Displayed with Quantum Dots. *RSC Adv.* **2015**, *5*, 93089−93094.
(132) Wu, M.; Petryayeva, E.; Medintz, I. L.; Algar, W. R. Quantitative Measurement of Proteolytic Rates with Quantum Dot-Peptide Substrate Conjugates and Förster Resonance Energy Transfer. *Methods Mol. Biol.* **2014**, *1199*, 215−239.
(133) Petryayeva, E.; Jeen, T.; Algar, W. R. Optimization and Changes in the Mode of Proteolytic Turnover of Quantum Dot-Peptide Substrate Conjugates through Moderation of Interfacial Adsorption. *ACS Appl. Mater. Interfaces* **2017**, *9*, 30359−30372.
(134) Goličnik, M. The Integrated Michaelis-Menten Rate Equation: Déjà Vu or Vu Jàdé? *J. Enzyme Inhib. Med. Chem.* **2013**, *28*, 879−893.
(135) Moreno, J. The Use of the Integrated Michaelis-Menten Equation in the Determination of Kinetic Parameters. *Biochem. Educ.* **1985**, *13*, 64−66.
(136) Marangoni, A. G. Characterization of Enzyme Activity. In *Enzyme Kinetics*; Marangoni, A. G., Ed.; 2003; pp 44−60.
(137) Purich, D. L. *Enzyme Kinetics: Catalysis & Control*; Elsevier: Boston, 2010.
(138) Briggs, G. E.; Haldane, J. B. S. A Note on the Kinetics of Enzyme Action. *Biochem. J.* **1925**, *19*, 338−339.
(139) Duggleby, R. G. Quantitative Analysis of the Time Courses of Enzyme-Catalyzed Reactions. *Methods* **2001**, *24*, 168−174.
(140) Kari, J.; Andersen, M.; Borch, K.; Westh, P. An Inverse Michaelis−Menten Approach for Interfacial Enzyme Kinetics. *ACS Catal.* **2017**, *7*, 4904−4914.
(141) Bajzer, Ž.; Strehler, E. E. About and Beyond the Henri-Michaelis−Menten Rate Equation for Single-Substrate Enzyme Kinetics. *Biochem. Biophys. Res. Commun.* **2012**, *417*, 982−985.
(142) Pons, T.; Medintz, I. L.; Wang, X.; English, D. S.; Mattoussi, H. Solution-Phase Single Quantum Dot Fluorescence Resonance Energy Transfer. *J. Am. Chem. Soc.* **2006**, *128*, 15324−15331.
(143) Díaz, S. A.; Malonoski, A. P.; Susumu, K.; Hofele, R. V.; Oh, E.; Medintz, I. L. Probing the Kinetics of Quantum Dot-Based Proteolytic Sensors. *Anal. Bioanal. Chem.* **2015**, *407*, 7307−7318.
(144) Yeh, F.-Y.; Tseng, I. H.; Chuang, S.-H.; Lin, C.-S. Spacer-Enhanced Chymotrypsin-Activated Peptide-Functionalized Gold Nanoparticle Probes: A Rapid Assay for the Diagnosis of Pancreatitis. *RSC Adv.* **2014**, *4*, 22266−22276.
(145) Wang, Y.; Liu, X.; Zhang, J.; Aili, D.; Liedberg, B. Time-Resolved Botulinum Neurotoxin a Activity Monitored Using Peptide-Functionalized Au Nanoparticle Energy Transfer Sensors. *Chem. Sci.* **2014**, *5*, 2651−2656.
(146) Sapsford, K. E.; Granek, J.; Deschamps, J. R.; Boeneman, K.; Blanco-Canosa, J. B.; Dawson, P. E.; Susumu, K.; Stewart, M. H.; Medintz, I. L. Monitoring Botulinum Neurotoxin a Activity with Peptide-Functionalized Quantum Dot Resonance Energy Transfer Sensors. *ACS Nano* **2011**, *5*, 2687−2699.
(147) Krishnamoorthy, K.; Hoffmann, K.; Kewalramani, S.; Brodin, J. D.; Moreau, L. M.; Mirkin, C. A.; Olvera de la Cruz, M.; Bedzyk, M. J. Defining the Structure of a Protein−Spherical Nucleic Acid Conjugate and Its Counterionic Cloud. *ACS Cent. Sci.* **2018**, *4*, 378−386.
(148) Jeen, T.; Algar, W. R. Mimicking Cell Surface Enhancement of Protease Activity on the Surface of a Quantum Dot Nanoparticle. *Bioconjugate Chem.* **2018**, DOI: 10.1021/acs.bioconjchem.8b00647.
(149) Wu, M.; Massey, M.; Petryayeva, E.; Algar, W. R. Energy Transfer Pathways in a Quantum Dot-Based Concentric FRET Configuration. *J. Phys. Chem. C* **2015**, *119*, 26183−26195.
(150) Algar, W. R.; Ancona, M. G.; Malanoski, A. P.; Susumu, K.; Medintz, I. L. Assembly of a Concentric Forster Resonance Energy Transfer Relay on a Quantum Dot Scaffold: Characterization and Application to Multiplexed Protease Sensing. *ACS Nano* **2012**, *6*, 11044−11058.
(151) Fu, J.; Liu, M.; Liu, Y.; Woodbury, N. W.; Yan, H. Interenzyme Substrate Diffusion for an Enzyme Cascade Organized on Spatially Addressable DNA Nanostructures. *J. Am. Chem. Soc.* **2012**, *134*, 5516−5519.
(152) Coley, C. W.; Barzilay, R.; Jaakkola, T. S.; Green, W. H.; Jensen, K. F. Prediction of Organic Reaction Outcomes Using Machine Learning. *ACS Cent. Sci.* **2017**, *3*, 434−443.
(153) Maryasin, B.; Marquetand, P.; Maulide, N. Machine Learning for Organic Synthesis: Are Robots Replacing Chemists? *Angew. Chem., Int. Ed.* **2018**, *57*, 6978−6980.
(154) Nielsen, M. K.; Ahneman, D. T.; Riera, O.; Doyle, A. G. Deoxyfluorination with Sulfonyl Fluorides: Navigating Reaction Space with Machine Learning. *J. Am. Chem. Soc.* **2018**, *140*, 5004−5008.
(155) Pardakhti, M.; Moharreri, E.; Wanik, D.; Suib, S. L.; Srivastava, R. Machine Learning Using Combined Structural and Chemical Descriptors for Prediction of Methane Adsorption Performance of Metal Organic Frameworks (MOFs). *ACS Comb. Sci.* **2017**, *19*, 640−645.
(156) Wexler, R. B.; Martirez, J. M. P.; Rappe, A. M. Chemical Pressure-Driven Enhancement of the Hydrogen Evolving Activity of Ni2p from Nonmetal Surface Doping Interpreted via Machine Learning. *J. Am. Chem. Soc.* **2018**, *140*, 4678−4683.
(157) Rodriguez-Perez, R.; Miyao, T.; Jasial, S.; Vogt, M.; Bajorath, J. Prediction of Compound Profiling Matrices Using Machine Learning. *ACS Omega* **2018**, *3*, 4713−4723.
(158) Smith, B. C.; Settles, B.; Hallows, W. C.; Craven, M. W.; Denu, J. M. SIRT3 Substrate Specificity Determined by Peptide Arrays and Machine Learning. *ACS Chem. Biol.* **2011**, *6*, 146−157.
(159) Yu, Z. L.; Casanova-Moreno, J.; Guryanov, I.; Maran, F.; Bizzotto, D. Influence of Surface Structure on Single or Mixed Component Self-Assembled Monolayers via in Situ Spectroelectrochemical Fluorescence Imaging of the Complete Stereographic Triangle on a Single Crystal Au Bead Electrode. *J. Am. Chem. Soc.* **2015**, *137*, 276−288.
(160) Mura, S.; Nicolas, J.; Couvreur, P. Stimuli-Responsive Nanocarriers for Drug Delivery. *Nat. Mater.* **2013**, *12*, 991−1003.
(161) Kelkar, S. S.; Reineke, T. M. Theranostics: Combining Imaging and Therapy. *Bioconjugate Chem.* **2011**, *22*, 1879−1903.
(162) Kamaly, N.; Yameen, B.; Wu, J.; Farokhzad, O. C. Degradable Controlled-Release Polymers and Polymeric Nanoparticles: Mechanisms of Controlling Drug Release. *Chem. Rev.* **2016**, *116*, 2602−2663.
(163) Pattni, B. S.; Chupin, V. V.; Torchilin, V. P. New Developments in Liposomal Drug Delivery. *Chem. Rev.* **2015**, *115*, 10938−10966.
(164) Zheng, T. T.; Li, G. G.; Zhou, F.; Wu, R.; Zhu, J. J.; Wang, H. Gold-Nanosponge-Based Multistimuli-Responsive Drug Vehicles for Targeted Chemo-Photothermal Therapy. *Adv. Mater.* **2016**, *28*, 8218−8226.
(165) Liu, H. Y.; Chen, D.; Li, L. L.; Liu, T. L.; Tan, L. F.; Wu, X. L.; Tang, F. Q. Multifunctional Gold Nanoshells on Silica Nanorattles: A Platform for the Combination of Photothermal Therapy and Chemotherapy with Low Systemic Toxicity. *Angew. Chem., Int. Ed.* **2011**, *50*, 891−895.
(166) Kumar, C.; Mohammad, F. Magnetic Nanomaterials for Hyperthermia-Based Therapy and Controlled Drug Delivery. *Adv. Drug Delivery Rev.* **2011**, *63*, 789−808.
(167) Pradhan, P.; Giri, J.; Rieken, F.; Koch, C.; Mykhaylyk, O.; Doblinger, M.; Banerjee, R.; Bahadur, D.; Plank, C. Targeted Temperature Sensitive Magnetic Liposomes for Thermo-Chemotherapy. *J. Controlled Release* **2010**, *142*, 108−121.
(168) Duan, C. C.; Liang, L. E.; Li, L.; Zhang, R.; Xu, Z. P. Recent Progress in Upconversion Luminescence Nanomaterials for Biomedical Applications. *J. Mater. Chem. B* **2018**, *6*, 192−209.
(169) Lee, N.; Yoo, D.; Ling, D.; Cho, M. H.; Hyeon, T.; Cheon, J. Iron Oxide Based Nanoparticles for Multimodal Imaging and Magnetoresponsive Therapy. *Chem. Rev.* **2015**, *115*, 10637−10689.

DOI: 10.1021/acs.langmuir.8b02733
Langmuir XXXX, XXX, XXX−XXX

(170) Delehanty, J. B.; Boeneman, K.; Bradburne, C. E.; Robertson, K.; Medintz, I. L. Quantum Dots: A Powerful Tool for Understanding the Intricacies of Nanoparticle-Mediated Drug Delivery. *Expert Opin. Drug Delivery* **2009**, *6*, 1091−1112.
(171) Friedlander, R. M. Mechanisms of Disease: Apoptosis and Caspases in Neurodegenerative Diseases. *N. Engl. J. Med.* **2003**, *348*, 1365−1375.
(172) Olsson, M.; Zhivotovsky, B. Caspases and Cancer. *Cell Death Differ.* **2011**, *18*, 1441−1449.
(173) Lopez-Otin, C.; Hunter, T. The Regulatory Crosstalk between Kinases and Proteases in Cancer. *Nat. Rev. Cancer* **2010**, *10*, 278−292.
(174) Olson, O. C.; Joyce, J. A. Cysteine Cathepsin Proteases: Regulators of Cancer Progression and Therapeutic Response. *Nat. Rev. Cancer* **2015**, *15*, 712−729.
(175) Martin, L.; Latypova, X.; Wilson, C. M.; Magnaudeix, A.; Perrin, M. L.; Yardin, C.; Terro, F. Tau Protein Kinases: Involvement in Alzheimer's Disease. *Ageing Res. Rev.* **2013**, *12*, 289−309.

DOI: 10.1021/acs.langmuir.8b02733
Langmuir XXXX, XXX, XXX−XXX